[redacted]

GPO PRICE $ _____

OTS PRICE(S) $ _____

Hard copy (HC) < 10

Microfiche (MF) .75

Coordinated Science Laboratory

UNIVERSITY OF ILLINOIS – URBANA, ILLINOIS

PROGRESS REPORT
FOR
JUNE, JULY & AUGUST, 1964

COORDINATED SCIENCE LABORATORY
UNIVERSITY OF ILLINOIS
URBANA, ILLINOIS

The research reported in this document was made possible by support extended to the University of Illinois, Coordinated Science Laboratory, under the Joint Services Electronics Program by the Department of the Army, Department of the Navy (Office of Naval Research), and the Department of the Air Force (Office of Scientific Research), and by the Advanced Research Projects Agency under Department of the Army contract

DA-28-043-AMC-00073(E)

the National Aeronautics and Space Administration under Grants

NsG 376 NsG 443 NsG 504

and Department of the Air Force (Office of Scientific Research) contract

AF 49(638) - 1383

November 9, 1964

COORDINATED SCIENCE LABORATORY

SUMMARY OF

PROGRESS REPORT FOR JUNE, JULY, AUGUST, 1964

1. Aerospace Group

Three rockets employing closed loop instrumentation for radio propagation measurements in the D region of the ionosphere were fired before, during, and after sunrise on July 15, 1964. Reduced data from the April 16 shot is presented.

2. Surface and Atomic Physics

Results of tests of an ultrahigh vacuum, rotary-motion, feedthrough are reported. An experiment to study the elastic and inelastic scattering of electrons at solid surfaces is described. A study of the cross-section for scattering and ionization of barium atoms by low energy electrons is reported. A summary of the progress on experiments to study the adsorption-desorption kinetics of gases at solid surfaces, the angular distribution of secondary electrons, and Auger electron ejection is given.

3. Computer Application Group

Continuing developments on an experimental time-sharing system are reported. Improvements and additions to the SMP-CSX-1 Bubble Chamber Data Processing work are described.

4. Systems

An important problem in the computer analysis of networks, namely the generation of trees without duplication, has been solved. The necessary and sufficient conditions for the realizability of a given state diagram as a quasi-linear sequential machine have been obtained. The necessary and sufficient conditions for the realizability of a given matrix as the A matrix (state matrix) of an RLC half-degenerate network have been found. The extension of the Dasher synthesis procedure into the right half plane is complete. Further progress is reported on the problems of the path matrix of a contact network, lossy communication networks, and self-diagnosing computers. New results in coding theory relate to the transmission rate in a communication channel. Several studies of nonlinear oscillating systems have been completed and are reported. In the area of control, progress is reported in studies of stability, system optimization, and rendezvous strategies.

5. PLATO

Progress on the construction and circuitry of the twenty student station teaching system indicates that at least ten student stations will be operable in November. The compiler, CATO (Compiler for Automatic Teaching Operation), has been completed. The resident program for CATO is now completely revised to allow for more efficient use of the PLATO III equipment, and compatibility with CATO-compiled programs. The inquiry training lesson, REPLAB, has been used further, this time by a demonstration class in a teacher's summer workshop on

inquiry training techniques. A short experiment in teaching small children the letters of the alphabet has suggested some of the problems involved in using PLATO with very young children. New lesson material under development includes a text book tester. The feasibility of externally controlled discharges has been successfully demonstrated in connection with the plasma discharge display tube research project.

6. Vacuum Instrumentation

Work on ultrahigh vacuum mass spectrometer studies is reported. Modifications to the photocurrent suppressor gauge show a considerable improvement in performance is possible. Some methods of repairing poor quality or damaged storage tubes are discussed. Impact ionization coefficients for CO on molybdenum and O_2 and CO on platinum are reported.

7. Plasma Physics

An algebraic theory of shock structure has been completed. The results of this theory and of recent Monte Carlo calculations have led to the preliminary design of a new numerical integration scheme for the Boltzmann equation. Theoretical work on oscillations in non-uniform plasmas was started. One particular model is discussed in some detail. The eigenvalues of oscillation are calculated explicitly.

8. High Magnetic Field Superconductors

Progress is reported in the following areas: (1) Preparation of single crystalline Nb_3Sn; (2) Studies of current peaks in the current-voltage characteristics of superconducting tunneling junctions related

to the AC Josephson effect; (3) Superconducting properties of thallium-antimony alloys; and (4) Development of a very sensitive low impedance voltage detector.

9. High Voltage Breakdown

The significance of critical field values for breakdown is discussed. Observations of emission points on broad electrodes, the effect of gas on prebreakdown currents, the use of gold electrodes, and further observations of field-emission flicker are reported.

10. Thin Films

Photoconductive measurements have been made on tin oxide films in the continuing effort to learn more about the electronic structure of this material. Using heated substrates, films of vanadium and niobium have been made which have normal superconducting properties. This is an important improvement over earlier results. The substrates were heated using an evaporated titanium film on the reverse side on the substrate as a resistive heating element. Electron diffraction and electron microscope photographs have been made of the structure of some tin films grown on cleaved NaCl substrates. Preliminary attempts have been made to deposit by evaporation luminescent screens.

11. Computer Operations

Operating statistics, equipment modifications, and systems programming are reported.

COORDINATED SCIENCE LABORATORY

Personnel

Faculty, Research Associates, and Research Engineers

Alpert, D., Director
Anderson, R.
Ash, R. B.
Barnard, H. M.
Bitzer, Donald
Böhmer, H.
Brown, R. M.
Chen, W. K.
Cooper, D. H.
Cruz, J. B.
Dodd, G.
Elliott, B.
Fenves, S.
Franz, Frank
Frauenfelder, H.
  Assoc. Director
Gentry, W.
Gooch, J.
Hicks, B. L.
Kirkwood, B.
Knoebel, H.
Kopplin, J. O.
Krone, H. V.
Kypta, L.
Lee, D. A.
Leichner, E. J.
Lichtenberger, W. W.
  (on leave)
Lüscher, E. (on leave)
Lyman, Elisabeth
Lyman, Ernest
Mayeda, W.
Mueller, T.
Peacock, R. N.
Perkins, W.
Ponzo, P.
Propst, F.
Prothe, W. C.
  Asst. to Director
Raether, M.
Resh, J.
Retherford, R. C.
Rohrer, R.
Satterthwaite, C. B.
Schuemann, W. C.
Seshu, Sundaram
Simonelli, L.
Skaperdas, D.
Slottow, H. G.
Sobral, M.
Steinrisser, F.
Stifle, J.
Tomaschke, H. E.
Trogdon, R.
Van Valkenburg, M. E.
  Assoc. Director
Voth, B.
Wax, Nelson

Research Assistants

Aggarwal, J. K.
Barger, A. R.
Batcher, K.
Bernstein, R.
Blomme, R.
Chang, Herbert Y.
Chen, W. K.
Cooper, T.
Craford, M.
Crowder, James
Cummings, James
Dervisoglu, A.
DeWan, E.
Gieseking, D.
Hosken, R.
Hummel, F.
Jacobs, J. T.
Jenks, Richard
Lie, T.
Manning, E.
McKellar, A.
Mendel, C.
Morgan, Lezlie
Murata, T.
Onaga, K.
Piper, Thomas
Secrest, M.
Smith, Margaret
Snyder, D. P.
Sobral, M.
Tahim, G.
Tibbets, G.
Toepke, I.
Werner, R.
Willson, R. H.
Zelac, R.

Fellows

Agashe, S.
Carr, W.
Paul, A.
Rain, D.
Sain, M.
Win, S.

Secretary

Gschwendtner, J.
Rudicil, J.

Accountant

Klein, N.

Typists and Stenos

Barnard, M.
Christy, L.
Harris, M.
Long, W.
Lucas, B.
McDonald, R.
VanCleave, C.

Instrument Makers

Beaulin, W. E.
Merritt, K. E.
Zackery, R. L.

Glassblower

Lawrence, W.

Phys. Sci. Staff Asst.

Thrasher, W.

Storekeepers

Drews, C. E.
Lofton, C.

Electronic Technicians

Casale, T.
Coad, D. E.
Cooper, G.
Crawford, G.
Deschene, D. R.
Holy, F. O.
Jordan, H.
Knoke, J. G.
Merrifield, F.
Roberts, G.
Schmidt, W.
Streff, L. W.
Turpin, F. G.

Accounting Clerk

Hanoka, Nila
Potter, R. E.

Photographer

Fillman, W.

Draftsmen

Conway, E.
MacFarlane, R. F.
Tewes, A. F.

Laboratory Mechanics

Bouck, G.
Burr, J. G.

Electronics Engr. Asst.

Carter, E. N.
Gardner, O. E.
Hedges, L.
Neff, E. H.
Vassos, N.

Res. Lab. Shop Supr.

Bandy, L.

Student Assistants

Alper, G.
Alpert, A.
Arnold, C.
Artman, J.
Bleha, W.
Chilton, S.
Edelheit, L.
Etienne, L.
Ewen, D.
Frampton, G.
Gibson, N.
Gobberdiel, J.
Hanson, A.
Johnson, M.
Jones, A.
Karr, G.
Klingbiel, R.
Metze, V.
Nagel, D.
Nash, R.
Riddle, G.
Ries, R.
Robinett, D.
Samson, C.
Sandorfi, G.
Singer, S.
Ulbrich, N.
Walker, M.
Whitney, R.
Klein, W.

PUBLICATIONS AND REPORTS

1. Journal Articles Published or Accepted

F. A. Franz and E. Lüscher, "Spin Relaxation of Optically Pumped Cesium," Phys. Rev. 135, A582 (1964).

2. Meeting Papers

Peter Braunfeld, "Computer-Based Teaching Systems as Aids to Human Reasoning," Symposium on Computer Augmentation, July 17, 1964, Washington, D. C.

J. B. Cruz, Jr. and W. R. Perkins, "The Role of Sensitivity in the Design of Multivariable Linear Systems," National Electronics Conference, October, 1964, Chicago, Illinois.

C. B. Satterthwaite, M. G. Craford, R. N. Peacock, and R. P. Ries, "DC Pair Tunneling between Two Superconductors at Finite Voltages," Ninth International Conference on Low Temperature Physics, August 31-September 4, 1964, Columbus, Ohio.

3. Technical Reports

R-218 Control of Co-operative Systems: The Rendezvous Problem; D. Gieseking.

R-219 Memory Effects in the Current-Voltage Characteristics of Thin Film Sandwiches; G. Riddle.

R-215 Role of the Generalized Lipschitz Condition in Finite-Time Stability and in the Derivation of the Maximum Principle; S. D. Agashe.

R-227 The Sensitivity of General Multivariable Feedback Systems; J. B. Cruz, Jr. and W. R. Perkins.

R-232 Anomalous Current Peaks in the I-V Characteristic for Tunneling between Two Superconductors; M. G. Craford, R. N. Peacock, R. P. Ries, and C. B. Satterthwaite.

TABLE OF CONTENTS

CONTENTS (Continued)

CONTENTS (Continued)

1. AEROSPACE GROUP

H. Knoebel
D. Skaperdas
B. Kirkwood
H. Krone
J. Gooch
G. Karr
W. Prothe
R. Anderson

On July 15, 1964, the Coordinated Science Laboratory fired three rockets of the Nike-Apache type in a series of experiments probing the ionosphere. This was conducted under a synoptic International Year of the Quiet Sun (IQSY) program which is directed by Dr. Sidney Bowhill. The experiments for which CSL was responsible were of a similar nature as the one conducted April 16, 1964, and reported in the CSL Progress Report for March, April, and May, 1964. The purpose of these propagation experiments is to measure the electron collision frequency profile of the D region for three different conditions; i.e., before, during, and after sunrise.

All three propagation experiments were successfully conducted in the closed loop mode, in which a servomechanism controls the extraordinary wave transmitted power, as explained in the previous progress report. In addition to all the signals which were telemetered from the rocket to the telemetry stations in the April 16 experiment, the receiver automatic gain control voltage was included in the three July 15 experiments. The availability of this information, together with rocket antenna and receiver calibration data, allows a determination of ordinary wave electric field intensity versus height to be made. It also allows corrections of the differential absorption profile for nonlinear receiver characteristics.

Since the sun's ultraviolet light is the main ionizing agent for the D region, conducting a series of rocket probes at precisely known intervals before and after sunrise provides for the measurement of the photoionization buildup due to the sun. Hence, one should observe very little differential absorption and Faraday rotation before sunrise as compared with after sunrise. The actual differential absorption and Faraday rotation data, versus time after launch, for rocket firing 14.144, during which the earth's shadow was up at about 330 Km, and for rocket firing 14.146, at which time there was no earth shadow at the launch area, are shown in Figures 1.1 and 1.2, respectively. The differential absorption data for flight 14.146 does show a higher trend than that for flight 14.144, but not very clearly. The reason for the large fluctuations is not presently known. Fluctuations of this magnitude were not observed in the differential absorption data for flight 14.143 fired April 16, 1964. The Faraday rotation data, on the other hand, shows clearly the expected dissimilarities between the two flights. In flight 14.144, the total Faraday rotation was approximately three cycles, whereas in flight 14.146 it was about 13-1/2 cycles. A puzzling fact is that the height at which the extraordinary wave was reflected in flight 14.143, as indicated by the abrupt rise in the corresponding differential absorption and Faraday rotation curves (82 seconds after launch, which corresponds to an altitude of about 50 miles) appears lower than that for flight 14.146, whereas the opposite should prevail.

Detailed data analysis is being continued on all four rocket firings in order to extract the maximum data. By means of

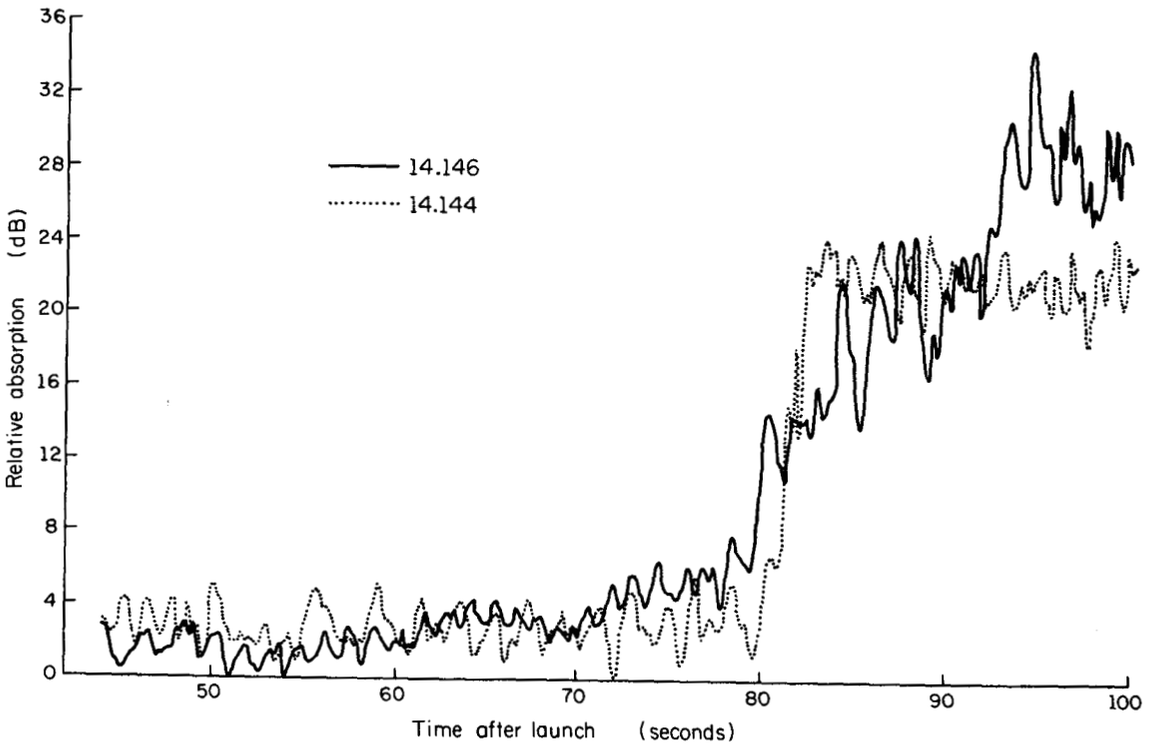

Figure 1.1. Absorption Data.

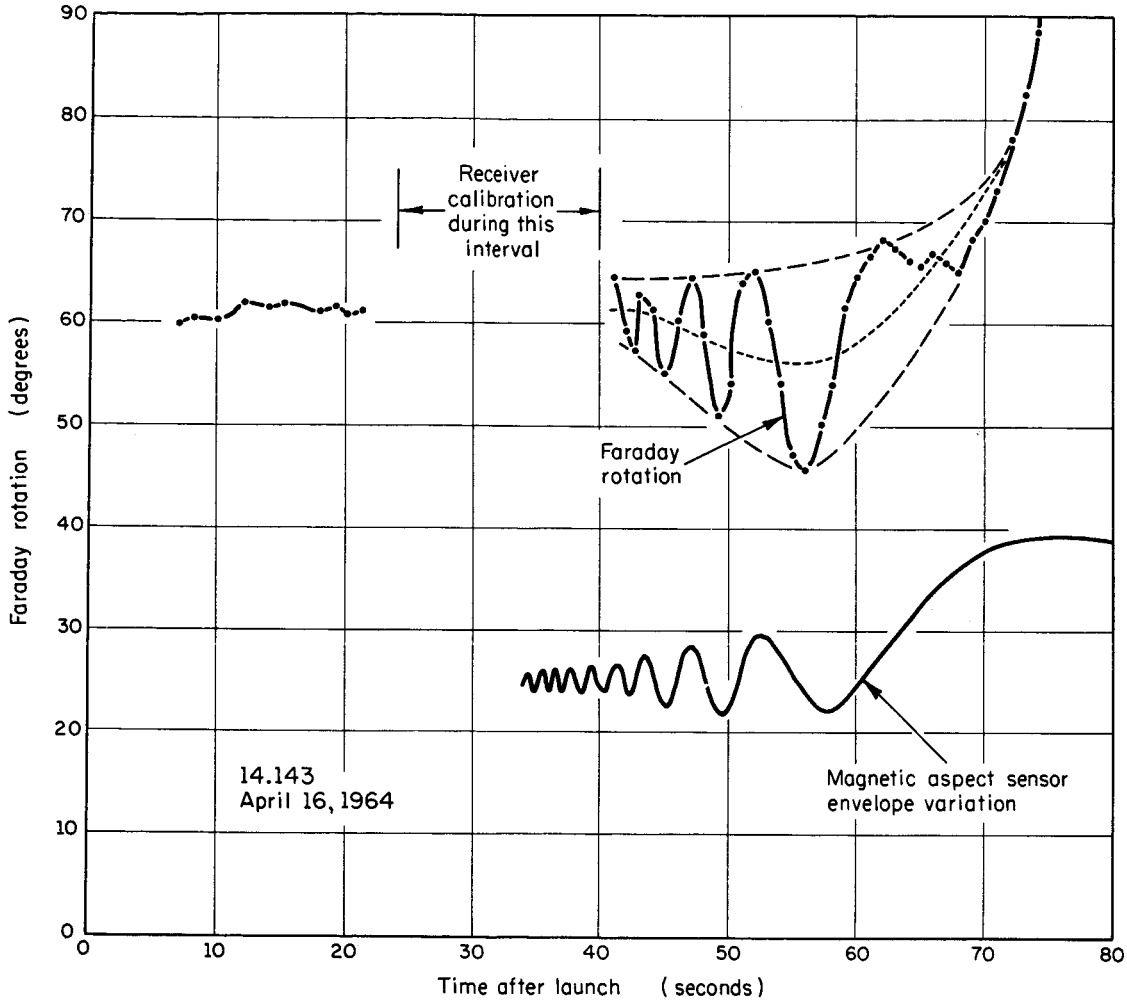

Figure 1.2. Faraday Rotation Data.

statistical analysis, Faraday rotation data is being extracted with a resolution of about one degree. In this way, a slight decrease with height in Faraday rotation before its larger monotonic increase may be concluded from the data shown in Figure 1.3 for flight 14.143. This data has been corrected for phase shifts which were introduced by the electronic circuitry used to extract the data from the telemetry tapes. Another circuit is being designed which should eliminate these phase shifts. In Figure 1.3 there is a very strong correlation with the rocket's precession about its trajectory path, as shown by the sketch of magnetic sensor envelope variation versus time.

A second van installation containing all the ground-based equipment except the antenna is being completed for use aboard an aircraft carrier. One of the firings aboard the carrier may take place at the earth's magnetic equator, at which the rocket trajectory would be transverse to the earth's magnetic field. For this transverse case a set of mutually perpendicular linearly polarized waves, instead of oppositely circularly polarized waves, would exhibit different indices of refraction with the resultant differential absorption and Faraday rotation. The use of mutually perpendicular linearly polarized transmitted waves places a greater burden on the rocket receiving antenna, which must be circularly polarized in order to receive both linearly polarized waves regardless of azimuth. Circuits to do this are now being tested.

D. Skaperdas

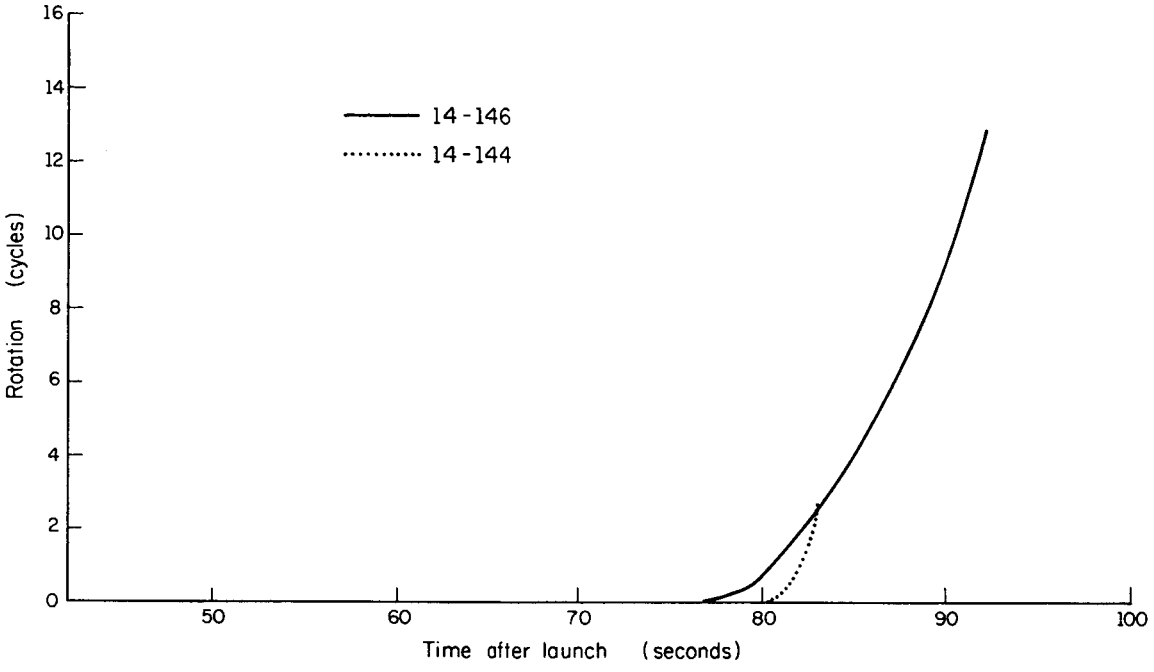

Figure 1.3. Faraday Rotation.

2. SURFACE AND ATOMIC PHYSICS

Surface:

F. Propst
R. Retherford
F. Steinrisser
L. Simonelli
T. Cooper
G. Tibbetts
T. Piper

Atomic:

H. Frauenfelder
F. Franz

2.1 Introduction

In the previous progress report, an experiment to study the angular distribution of electrons ejected by ions and by electrons striking a solid surface and an experiment to study the adsorption-desorption kinetics of gases at solid surfaces were described. The design of these two experiments is essentially complete and the apparatus is being constructed. It is possible that both of these systems will be assembled during the next quarter.

An instrument designed to study the scattering of electrons from solid surfaces has been designed. It is felt that this technique is potentially very powerful in that a large number of processes can possibly be studied by it. In addition, it may also be possible to study ion emission by electron impact using this system. Since high resolution (0.1 V) is possible, these experiments may prove to give substantial data amenable to theoretical analysis--a sorely needed commodity in the area of surface science. This system is described in greater detail below.

The apparatus used in the study of Auger electrons (these experiments and results have been presented in several previous progress

reports) has been modified, and work in this area is continuing. In addition, the scattering of ions from solid surfaces will be investigated in this system.

2.2 Rotary-Motion Feedthrough

The ultrahigh vacuum, rotary-motion feedthrough[1] described in the previous progress report has been constructed. The output shaft was lubricated with dry MoS_2 powder.[2] A vacuum of about 5×10^{-10} Torr was obtained using a small oil pumped system. The exterior bearings were water cooled during bakeout. Pressure increments from 2×10^{-10} Torr to 5×10^{-8} Torr were observed corresponding to angular speeds from 1 RPM to about 50 RPM.

It is expected that the vacuum can be improved by removing the exterior bearings and using a clamp for bakeout instead of water cooling. This will allow the bellows and output bearings to be baked at a higher temperature.

T. Cooper

2.3 Electron Scattering at Solid Surfaces

2.3.1 Introduction. Indirect evidence that electrons lose energy in discrete amounts in interacting with the surface region of solids is given by studies of the Auger electron energy distribution[3] (caused by slow He ions incident on solid surface) for surfaces with

---

[1] Progress Report for March, April, May, 1964. Section 2.2, page 26: Angular Distribution of Auger Electrons.

[2] The MoS_2 powder was obtained from the Moly-Kote Company.

[3] F. M. Propst and E. Lüscher, Phys. Rev. 132, 1037 (1963).

varying adsorbate coverage. Studies of the photo-electric electron energy distribution emerging from surfaces of varying adsorbate coverage yield similar evidence.[4] An energy loss mechanism has been used to partially explain the energy distributions obtained. However, little of positive nature can be learned of this, and other loss mechanisms which may be involved, by studying the energy distribution of electrons emerging from the surface of a solid which is stimulated by either the Auger or photo-electric process. The electron energy distribution which is produced within the solid by either the Auger or the photo-electric process is very broad, the width of the electron energy distribution being of equal magnitude to the maximum electron energy involved. Thus, any energy loss mechanism which may be present will not be resolved and can only be detected by the shifts which they cause in this broad energy distribution.

The electron energy loss mechanism invoked to explain the difference between the Auger distribution for a clean W surface and that of a W surface with a gas adsorbed is[3] that, when electrons originating from the Auger process reach the surface of the solid, some stimulate electrons in the ground state levels of the adsorbed gas to jump to higher levels. In this process, the energy of the Auger electron is lowered by a discrete amount U, the energy which is taken up by the electron associated with the adsorbed gas atom or molecule. The net visible effect of this upon the Auger electron energy distribution of a clean surface is a decrease in the distribution at the high energy

---

[4] C. N. Berglund, Tech. Rep. No. 5205-1, Center for Materials Research.

end and an increase in the distribution in the lower energy region. Further, since all Auger electrons which excite electrons of the adsorbed gas must be displaced in the energy distribution to a point of energy at least the amount U below their original energy, the distributions for clean and gas-adsorbed surfaces should be of the same shape (one should be able to get one from the other by simply using the correct multiplying factor) from the high energy cut-off, E_o, down to energy E_o-U. This is found to be true experimentally. Also, it is indicated that the multiplier necessary to make the adsorbed-gas Auger distribution coincide with the clean-surface Auger distribution in the range from E_o-U to E_o is directly proportional to the adsorbate coverage.

The same mechanism can be used to explain the difference between the photo-electric distribution for a clean and an absorbate covered surface.

There are many energy loss mechanisms other than the electronic transitions of an adsorbed gas which also make discrete electron energy loss transitions possible. However, most of these cannot be "turned on" and "turned off" by adsorbing and flashing-off an adsorbable gas as can the electronic transitions of an adsorbed gas, so that their shifting effect on the broad energy distribution of the Auger and photo-electric process cannot be detected; nevertheless, it is quite likely that they are present. Some of the energy-loss mechanisms which could cause electron energy losses are the following:

A. Studies by Gomer[5] on surface ionization of adsorbed CO indicate that molecular vibration levels can be excited. Since these are separated by only roughly 1/10 volt, they will be even more difficult to "see" than the adsorbate electronic levels which have level separations of roughly 10 volts. Suppose that the adsorbate was stimulated by a "monochromatic" electron beam of total half width 1/45 volt incident on target surface and that the resultant "reflected" beam was energy analyzed with the same 1/45 volt resolution, then one hopefully should be able to see a set of peaks separated from the incident energy by the vibrational energy level separations (since the over-all energy resolution is less than 1/25 volt which is less than 1/10 volt).

B. In semiconductors, studies of surface conduction have established the existence of "potential troughs" at the surface of the semiconductor. The existence of the surface states in these potential troughs, their width, and their exact location could be further established by using the same technique suggested above for the study of the vibration levels of adsorbed CO.

C. Acceptor and donor levels provide energy levels which make discrete electron-energy loss transitions possible. Even though these levels are in the bulk material, this could possibly be studied as suggested in A and B.

---

[5] R. Gomer and L. Swanson, J. Chem. Phys. 39, 2833 (1963).

D. The first, second, and etc., filled bands below the conduction band of a metal provide energy levels which can cause electrons in an incident beam to lose energy. Several types of electron energy transition occur if the incident beam has enough energy to excite electrons from these filled bands: (a) the electron initially excited may be set free or end-up in the conduction band; (b) an electrpn from the conduction band will fall into the hole exciting an Auger electron from the conduction band; (c) etc.

2.3.2 Experimental Apparatus. The experimental apparatus proposed and now under construction to study these energy loss mechanisms is a set of electrostatic energy analyzers and the necessary related apparatus. The electrostatic energy analyzers shown in Figure 2.1 consist in essence of portions of concentric cylinders with a difference of potential between. The magnitude of the potential between the two portions of cylinders determines the energy of the electrons that can pass through the analyzer. The width of the slits at either end of an analyzer determines to a large degree the energy resolution of the analyzer. The optimum energy resolution of each of the analyzers being constructed is $2\Delta V/V = 1/45$.

A single crystal of tungsten will be the first target used. A careful energy analysis of the electrons "reflected" from the surface of the target as it is bombarded with "monochromatic" electrons for both clean and gas adsorbed targets should allow one to make some direct and meaningful statement concerning the energy loss mechanisms at work.

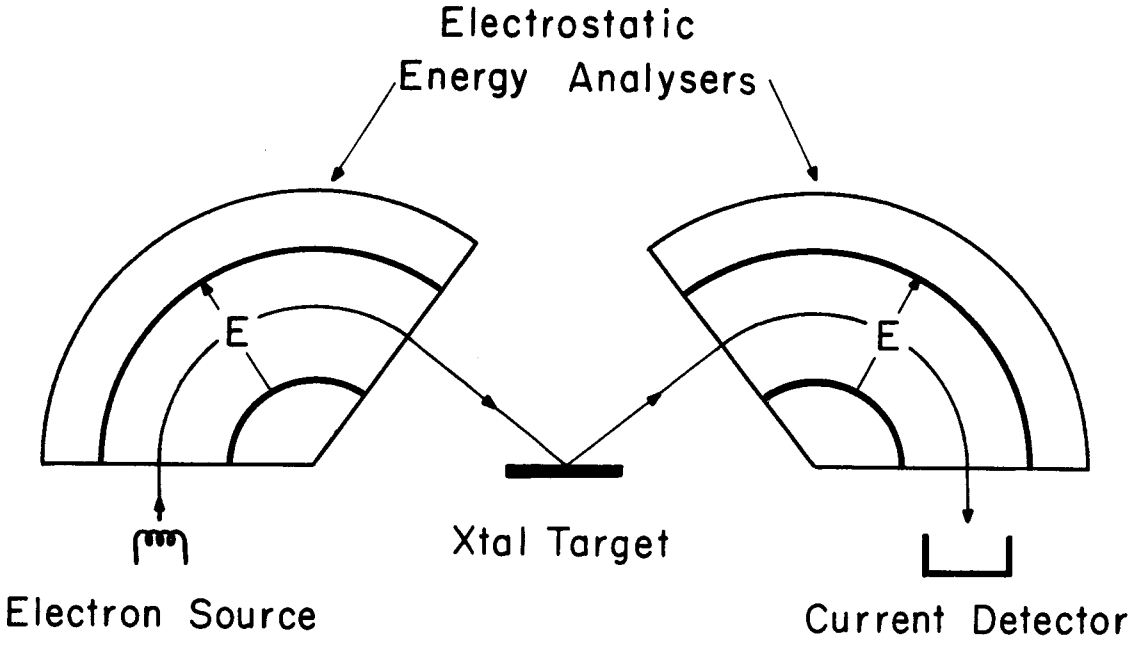

Figure 2.1. Schematic of Electron Scattering Apparatus.

2.4 Total Cross-Sections for Scattering and for Ionization of Barium Atoms by Low Energy Electrons

Very little data exists in the literature on the properties of barium as a plasma constituent. No reference has been found, for instance, to measurements of collision cross-sections or to excitation functions. This lack of information about barium and other alkaline earth elements may be ascribed to their low vapor pressures as compared to the alkalies and to zinc, cadmium, and mercury, all of which have been studied in some detail. However, advances in materials technology have made it possible to contain barium vapor, and an experimental barium-plasma device was reported recently by Kennedy, Shefsiek, and Talaat.[6] This is a thermionic energy converter in which barium ions are employed to neutralize the electronic space-charge. The results show that the ionizability of barium vapor, although not as great as for cesium vapor, is sufficient to provide the ions needed for neutralization in a thermionic converter. The degree of ionization is substantially greater than predicted from the ionization potential and the Saha-Langmuir formula. This suggests that the metastable states in barium, for which spectroscopic evidence exists, must play an important role in producing the ions. However, this role will remain essentially speculative until certain fundamental data are obtained. The immediate objective of this investigation is to obtain experimental

---

[6] A. J. Kennedy, P. K. Shefsiek, and M. E. Talaat (Martin Company, Nuclear Division),"Research and Development for Barium Vapor-Filled Thermionic Energy Conversion Technology." Summary Report MND-2933-2 (May, 1964).

information on total collision cross-sections for scattering and for ionization of barium atoms in collisions with low energy electrons. Plans have been made for extending the investigation to include excitation cross-sections of the metastable states at an appropriate time.

An atomic beam method will be used in the study. The essence of the method is illustrated schematically in Figure 2.2. A narrow beam of barium atoms is produced by an oven and collinating slit. The beam is cross-fired by a stream of slow electrons of known energy, thereby producing scattering of both electrons and barium atoms, and in addition excitation and ionization when threshold energies are exceeded.

The total cross-section for ionization is the simplest from the viewpoint of detection. A suitable positive ion collector can be used to count the ions.

The total cross-section for scattering by slow electrons will be determined by a method similar to that used by Rubin, Perel, Bederson and Englander in measurements of cross-sections of alkali atoms.[7] If the acceptance width of the beam detector is less than the beam width, scattering collisions deplete the detected beam intensity, thereby permitting the collisions to be counted. A surface ionization detector described by Hay[8] will be used to detect the barium atoms.

---

[7] Phys. Rev. 117, pp. 151-158 (1960), and Phys. Rev. 128, pp. 1148-1154 (1962).

[8] R. H. Hay, "The Nuclear Magnetic Moments of C^{13}, Ba^{135} and Ba^{137}," Phys. Rev. 60, pp. 75-86 (1941).

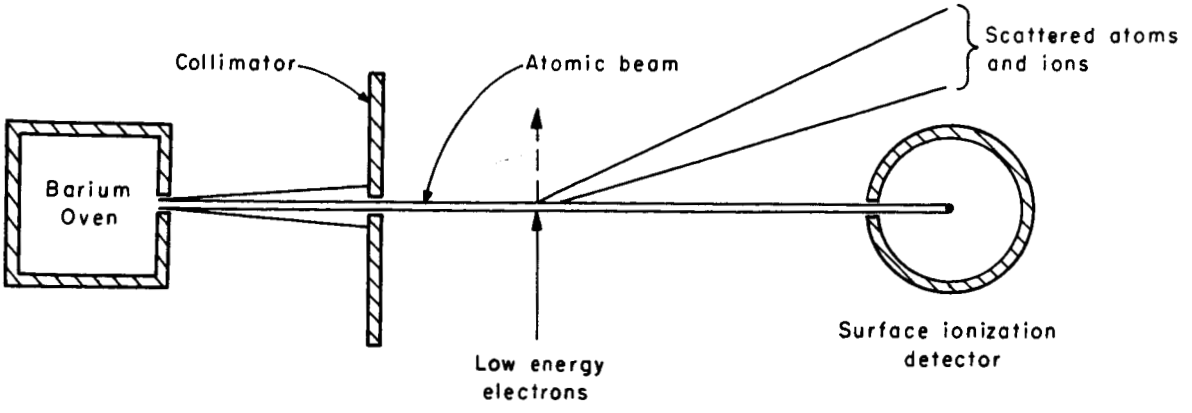

Figure 2.2. Schematic of the Apparatus for the Study of the Electron Scattering from Barium Atoms.

Close control of surface conditions is essential for the functioning of the surface ionization detector and for the detection scheme under consideration for metastable barium atoms. The investigation of surface effects in these detectors is an important aspect of the program. Consequently, the study will be carried out under ultrahigh vacuum conditions.

Preliminary plans have been made for the entire study. Construction of components of the apparatus will be started shortly.

R. Retherford

3. COMPUTER RESEARCH APPLICATIONS

R. M. Brown
S. Fenves
R. Trogdon
J. Stifle
R. Jenks

3.1 Introduction

This group is concerned with the design and applications of digital computers for information processing, primarily in the areas of real-time and non-numerical operations. The present work concerns the development of an experimental time-sharing system and studies in the applications of computers in experimental physics.

3.2 Logical Design

The designer of digital data processing equipment invariably finds himself dealing with Boolean expressions which describe the functions and operations performed by the equipment. More often than not, these expressions may be simplified, yielding simpler and more economical circuits. Although there are many well known techniques for simplifying Boolean expressions, even the best of these techniques can be quite time consuming, especially if a large number of variables is involved.

To eliminate this time-consuming operation, a program has been written for the CSX-1 which can be used to simplify Boolean expressions containing up to eight variables. The program uses the iterated consensus technique first described by Shannon and Mills.

A description of this technique may be found in "Theory and Design of Digital Machines," by Bartee, Lebow, and Reed, Chapter 4, Sections 4.1 to 4.8 (McGraw-Hill, 1962).

J. Stifle

3.3 The DIOG Experimental Time-Sharing System

During the previous quarter, hardware has been installed in the CSX-1 to handle the communication between 7094 and the CSX-1 for the proposed DIOG system (see Progress Report for March, April, May, 1964). This equipment employs five CSX-1 input-output channels; three channels provide for data transfer to and from the 36-bit-word memory of the 7094 while the other two channels are used for control information. This equipment makes the DIOG system compatible with the existing 7094 system written by the Digital Computer Laboratory, eliminating the need for any special program interface between the 7094 system program and the input-output channels.

The Phase Zero DIOG Program has been completed and checked out by simulation. In Phase Zero, the user operates in one of two modes. In the executive mode, a dialogue is carried out between the user at the console flexowriter and the CSX-1 for the purpose of specifying and activating a desired functional program in the 7094. Four directives or commands may be given to the DIOG control program in the executive mode: "LOGIN" initiates a dialogue; "CALL" enables the user to specify an on-line functional program; "TERMINATE" is used to terminate the dialogue with the previously called functional program; "LOGOUT" closes out a dialogue.

Following the establishment of a program, the user and CSX-1 enter the program mode where the CSX-1 transmits messages back and forth between 7094 and the user. Here messages are accumulated by the CSX-1 and monitored for one of two signals: (1) a "carriage return" character which causes the transmission of the previously entered line to the 7094; (2) a "STOP" character flexowriter which produces a transfer of the dialogue back to the executive mode. Further details of the DIOG system are given by internal memo D2.

Initial Phase Zero checkout with the 7094 will involve only data transmissions between the two computers with the monitor system in the 7094 simulated in the CSX-1. Further Phase Zero checkout awaits changes in the existing 7094 executive system which will allow the 7094 to operate either in the on-line mode or the conventional batch processing mode.

R. M. Brown
R. Jenks

3.4 SMP Bubble Chamber Data Processing

The SMP measuring console has been moved to the Physics Building and a communication line to the CSX-1 computer installed. In the coming months three more units will be added and multiplexed to the CSX-1. The measuring program, DMSCAMP, is in the process of modification to permit measurements on film from the Argonne 30" chamber concurrent with measurements on Berkeley 72" chamber film. Significant improvements have been made in the accuracy of the data processing and the incorporation of console diagnostic procedures.

R. M. Brown

4. SYSTEMS

Circ. & Commun.	Control Systems	Switch. Systems
M. E. Van Valkenburg	J. B. Cruz, Jr.	S. Seshu
J. K. Aggarwal	S. D. Agashe	K. E. Batcher
R. B. Ash	D. Gieseking	A. Dervisoglu
D. H. Cooper	T. E. Mueller	G. Dodd
P. Ponzo	T. Murata	B. Elliott
R. A. Rohrer	W. R. Perkins	W. Mayeda
N. Wax	R. A. Rohrer	K. Onaga
	D. Snyder	A. Paul
	G. Tahim	J. A. Resh
	R. Werner	H. Y. Chang

4.1 Generation of Trees without Duplication

One of the important problems in the implementation of computer methods of network analysis is the generation of the trees of a linear graph without duplication. Further, in order to be able to compute the sign of a tree (which has to be done in the analysis of active networks) the trees must be generated by replacement of one branch at a time. A tree generation scheme satisfying these requirements has been obtained and has been reported in report number R-220. In this procedure duplications are avoided by two devices. On the one hand, we arrange the branches of the starting tree into an ordered sequence such that any leading subset of branches in the sequence constitutes a connected subgraph. On the other, we require that any link which replaces a branch of the present tree belong not only to the fundamental cut-set of the replaced branch with respect to the present tree (which is necessary in order that the new set of branches be a tree) but also to the fundamental cut-set of the branch with respect to the starting tree. The

replacement is also ordered left to right in the ordered sequency representation of the starting tree. It has been shown that this scheme generates all the trees of the graph and no tree is generated more than once.

The detailed procedure and the proofs of the assertions above are to be found in the cited report.

W. Mayeda
S. Seshu

4.2 Quasi-Linear Sequential Machines

The investigation on the realizability of quasi-linear sequential machines has been completed. A necessary and sufficient condition was obtained for a given connection matrix (or a state diagram), with the given encoding of states, to be realizable as a quasi-linear sequential machine making use of minimal number of feedback lines. Also obtained was a canonical realization which enables one to realize any arbitrary state diagram as a quasi-linear sequential machine using a sufficiently large number of memory elements. These results are discussed in detail in Report R-216.

The invariant properties of the state diagram of quasi-linear sequential machines, with respect to the change of coding of states, are being studied.

H. Y. Chang

4.3 Self-Diagnosis

Work has been started on a problem of self-diagnosis; the object of study is the laboratory's CSX-1 computer. Initial attempts

to devise a bootstrap diagnostic procedure (no external testing device, none of the machine assumed error-free a priori) have been encouraging. The primary tool used is the SEQANALZ (Report R-207) system of programs.

E. Manning

4.4 Synthesis of Sequential Machines

A new method for the synthesis of asynchronous sequential machines is being developed. The most novel feature of this procedure is that it breaks the problem of finding a realization of a given flow table into a series of smaller problems in a manner somewhat analagous to the synthesis of conventional one terminal-pair electrical networks. Further, the procedure is suited to machine computation.

An algorithm is being developed in connection with this synthesis procedure which will attempt to obtain state assignments with reduced dependency. Particular emphasis is being placed on obtaining cascade realizations because of the engineering advantages they enjoy.

A. McKellar

4.5 Directed Graph Synthesis

The study of directed graphs and their application to synthesis of switching networks was continued. Some operations on a connection matrix which leave the associated output matrix invariant were formulated. The relationship between the number of directed paths between two distinguished vertices and the nullity of the graph is being studied.

A. Paul

4.6 Lossy Communication Nets

A structure of basic saturated cut sets of a lossy communication net is being investigated. Synthesis procedures of $\overline{T}$ and $\underline{T}$ matrices of a lossy, bi-complete tree net have been derived.

K. Onaga

4.7 A-Matrix Synthesis

Necessary and sufficient conditions for a matrix to be realizable as the A-matrix of an RLC network are developed. The RLC network is assumed to be non-degenerate or half-degenerate and it is assumed to have a connected resistive part.

The resistive part N_R and the reactive part N_X of the RLC network are considered separately. It is shown that if there exists a realization then the given matrix A can be factored as $-\Lambda A_1$ where Λ is a diagonal matrix of positive entries and A_1 is a symmetric-skewsymmetric (hybrid) matrix. The matrix Λ determines directly the values of capacitances and inductances in the network. A technique is given by which the terminal matrix of the resistive part N_R and the fundamental circuit matrix of the reactive part N_X can be obtained from the matrix A_1.

It is shown that the given matrix A has a realization with a half-degenerate or non-degenerate RLC network which has a connected resistive part if and only if the factorization exists and both the terminal matrix and the circuit matrix are realizable. It is also shown that for a certain factorization if a realization exists, then the reactive part is unique within two-isomorphism and the resistive part

can always be reduced to a complete polygon in general. The synthesis technique applies to the case where inductances and capacitances are time dependent but resistances are time independent. These and other results are presented in CSL Report R-225, July, 1964. An extension to the degenerate case is being studied.

A. Dervisoglu

4.8 Dasher Synthesis

The extension of the Dasher synthesis procedure (realization of complex transmission zeros by means of cascaded RC networks) to zeros in the right half plane in the sector

$$\pi/3 < |\arg s| < \pi/2$$

is now complete. The conditions to be satisfied by the driving point function have all been derived as inequality constraints thus simplifying the preparation problem. The section used in the synthesis procedure is the simplest possible section which is capable of realizing transmission zeros in the desired sector. The procedure for converting the unrealizable section which results in this process into a realizable section using the Baker node insertion process has also been derived.

The detailed description and justification of the procedure have been reported in report R-231.

B. Elliott

4.9 Distributed Network Synthesis

Most of the time this summer has been spent on the development of a digital computer program to implement the time-domain distributed-network synthesis method originated by Professor Rohrer. Although it is not yet completed, the major difficulties appear to have been ironed out; of course, evaluation of the iterative scheme being employed will have to be deferred until the program is working--I see no path toward an *a priori* convergence proof.

J. Resh

4.10 Coding Theory

An aspect of coding theory called the *strong converse* is being considered. This result states that if the transmission rate of a communication channel is maintained above capacity, the probability of error of an optimal code approaches unity as the code word length approaches infinity (Shannon's fundamental theorem implies only that the probability of error cannot approach zero) the strong converse does not hold for all channels, as has been found by Wolfowitz. The problem now being investigated involves finding the essential feature of a channel which determines whether or not the strong converse should apply. Preliminary investigation has shown that a channel need not be very complicated for the strong converse to fail; for example, a channel whose inputs and outputs are binary sequences of length n, with transmission errors uniformly distributed between 0 and n, does not obey the strong converse. This result is proved, and some estimates of the relationship

between transmission rate and probability of error are derived, in a paper submitted to the IEEE Transactions on Information Theory.

R. Ash

4.11 Nonlinear Oscillating Systems

Various studies of oscillating systems have been completed this quarter. Three laboratory reports were issued and a short manuscript written during the period. Two of these reports (R-228 and R-229) have been submitted to the journals, and the short manuscript (see 4.11.4) has already been accepted for publication. Abstracts of the work are given below:

4.11.1 J. K. Aggarwal, "A Study of Nonlinear Second Order Systems," R-223.

Nonlinear second order systems, which are described by a pair of coupled first order differential equations, have been studied. The behavior of trajectories in the neighborhood of a singular point and the behavior of trajectories in the large have been examined.

The isolated singularity at the origin for the system

$$\dot{x} = ax^{n1} + by^{n2}$$
$$\dot{y} = cx^{n3} + dy^{n4}$$

where a, b, c, and d are real, and n_1, n_2, n_3, and n_4 are positive integers, has been investigated. Sufficient conditions for the stability and instability of the singular point have been found.

The global behavior of the systems

$$\dot{x} = -f(x) + g(y) + p(t)$$

$$\dot{y} = -h(x)$$

and

$$\dot{x} = -f(x) \pm g(y) + p(t)$$

$$\dot{y} = \pm h(x) - k(y) + q(t)$$

has been investigated. Here $f(x)$, $g(y)$, $h(x)$, and $k(y)$ are polynomials of odd degree with leading coefficients positive, and $p(t)$ and $q(t)$ are periodic bounded functions of time. Sufficient conditions have been found under which the trajectories of the above systems may eventually be confined in a subset of (x,y,t)-space, thus giving bounds on periodic solutions (if they exist). Further, bounds on the periodic solutions have been investigated by finding regions in (x,y,t)-space from which all trajectories eventually leave, and into which no trajectories enter. Also, other bounding curves for the generalized Rayleight equation have been investigated.

4.11.2 P. J. Ponzo and N. Wax, "On Certain Relaxation Oscillations: Confining Regions," R-228.

Relaxation oscillations described by the generalized Liénard equation, $\ddot{x} + \mu f(x)\dot{x} + g(x) = 0$ ($\cdot \equiv d/dt$), with $\mu \gg 1$, are investigated in the phase and Liénard planes. When $f(x)$, $g(x)$, and $F(x) = \int_0^x f(u)du$ are subject to certain restrictions, a number of analytic curves can be obtained in these planes which serve as bounds on solution trajectories. Piece-wise connection of such bounding curves provide explicit annular regions with the property that solution

trajectories on the boundary of an annulus move to the interior with increasing time, t. The Poincaré-Bendixson theorem then guarantees at least one periodic orbit within such an annulus. It is shown that the periodic orbits which are isolated by this means are unique within the annulus, hence orbitally stable. The maximum width of the annulus is of order $\mu^{-4/3}$; the amplitude bounds obtained for the periodic solution agree favorably with the known amplitude for the specific case of the van der Pol equation $\ddot{x} + \mu(x^2-1)\dot{x} + x = 0$. The results are generalized to less restrictive f(x), g(x), and F(x) than those first considered.

4.11.3 P. J. Ponzo and N. Wax, "On Certain Relaxation Oscillations: Asymptotic Solutions," R-229.

Periodic solutions of the generalized Liénard equation $\ddot{x} + \mu f(x)\dot{x} + g(x) = 0$ ($\cdot \equiv d/dt$), with $\mu \gg 1$, are investigated in the phase and Liénard planes. Certain comparison equations are obtained by modifying the functions f(x), g(x), $F(x) = \int_0^x f(u)du$, so that the resulting equations may be integrated to within an error of order μ^{-2}. The comparison solutions are used to approximate the solution trajectories of the original equations, and, in particular, the periodic orbits. The result is an analytic description of the trajectories, in both planes, to order μ^{-2}. The asymptotic form of the amplitude and period, for a periodic orbit, is obtained with errors of order μ^{-2} and μ^{-1}, respectively. For the particular case of the van der Pol equation, $\ddot{x} + \mu(x^2-1)\dot{x} + x = 0$, the amplitude agrees with the expressions previously obtained by other workers, while the period does not. The results of a numerical study of the expression for the period given here support the present work.

4.11.4 P. J. Ponzo and N. Wax, "On the Periodic Solution of the van der Pol Equation."

The general results of R-229 have been particularized to the van der Pol equation. Our analytical results do not agree with other formulas for the period. We have computed the period numerically using the laboratory's CDC 1604 and established the validity of our results.

J. Aggarwal
P. Ponzo
N. Wax

4.12 Finite-Time Stability and Maximum Principle for Systems Satisfying a Generalized Lipschitz Condition

In CSL Report R-215, differential controlled processes satisfying a generalized Lipschitz condition were considered. Such processes are a generalization of time-varying linear processes. Some conditions regarding the existence of a solution of the differential equations describing the process and existence of varied solutions, and upper bounds for variations of the solution were pointed out.

It was shown that if a system satisfies a generalized Lipschitz condition in the state variables, it is finite-time stable with respect to the initial state. If it satisfies a generalized Lipschitz condition in the control as well, it is finite-time stable with respect to the control also.

A new derivation of the Pontryagin Maximum Principle and the Transversality Condition as necessary conditions for a local extremum (and, hence, for a global optimum) was given. This follows a calculus of variations approach but uses the Lagrange multipliers in a different

way. It was shown that if a generalized Lipschitz condition in the state variables and the control is satisfied, and also another condition is satisfied, for sufficiently small but arbitrary variations of the optimum control, the terminal conditions of the problem can still be met.

S. Agashe

4.13 Linear Time Lag Systems

The concept of complete controllability has been extended to the case of linear time invariant systems with time lags. Through this the study of the relationship between the frequency domain analysis of time lag systems and the optimal control theory is being made. The sensitivity of the multivariable time lag systems has been investigated from the point of view of Cruz and Perkins.[1]

G. Tahim

4.14 Stochastic Optimal Control

Initial investigations, reported previously, have been extended to a class of continuous-time, multivariable, noisy control systems.

Studies have focused on a particular type of functional, and have led to the definition of related performance criteria. The nature of the corresponding optimal control has been investigated numerically for specific examples, and analytically for a sub-class of these problems.

---

[1] J. B. Cruz and W. R. Perkins, "A New Approach to the Sensitivity Problem in Multivariable Feedback System Design." Presented at J.A.C.C., Stanford (June, 1964).

Analytical studies are being broadened, numerical techniques are being formulated, and results are being generalized to discrete-time systems.

M. Sain

4.15 Optimum Time Lag Systems

It has been shown by N. N. Krasovskii[2] that the optimum feedback controller for a time lag system described by

$$\dot{\underline{x}}(t) = A(t)\underline{x}(t) + B(t)\underline{x}(t-h) + C(t)\underline{u}(t)$$

and minimizing

$$J = \int_o^T [\underline{x}^T(t)Q\underline{x}(t) + \underline{u}^T(t)R\underline{u}(t)]\, dt$$

has the form

$$\underline{u} = \alpha(t)\underline{x}(t) + \int_{-h}^{o} \beta(t,\tau)\underline{x}(t+\tau)\, d\tau$$

where $\alpha(t)$ and $\beta(t,\tau)$ are matrices.

The numerical solution for α and β is difficult. A gradient technique is being developed to find α and β by forcing a closed loop solution rather than the standard open loop solution used in conventional gradient techniques.

T. Mueller

---

[2] Krasovskii, N. N., "Analytic Construction of an Optimal Regulator in a System with Time Lags," PMM Vol. 26, No. 1 (1962).

4.16 Optimum Control with a Prescribed Structure

The following two problems are being investigated. Given the optimum control problem

$$\dot{\underline{x}} = \underline{f}(\underline{x},\underline{u},t)$$

$$\underline{x}(t^o) = \underline{x}^o \ , \qquad \text{final T given}$$

$$J(u) = \int_{t^o}^{T} h(\underline{x},\underline{u},t)\ dt$$

(a) find a function $\underline{g}(\underline{x},\underline{u},t)$ [at least approximately] such that

$$\dot{\underline{u}} = \underline{g}(\underline{x},\underline{u},t), \qquad \underline{u}^o \text{ to be chosen}$$

yields an optimum control;

(b) find matrices A(t) and B(t) [at least approximately] such that

$$\dot{\underline{u}} = A(t)\underline{x} + B(t)\underline{u}$$

yields an optimum control.

Translation of the book "Fondamenti di Calcolo delle Variazioni" (Fundamentals of the Calculus of Variations) by L. Tonelli is under way. This book introduces certain concepts that have not yet been exploited well and that make the Calculus of Variations a proper sub-area of functional analysis.

S. Agashe

4.17 Pulse-Width Modulation Systems

The problem of optimal open-loop control for a system containing a pulse-width modulator has been solved by the method of the steepest-ascent method, and possible utilization of other methods are presently under investigation.

D. Kirk

4.18 A Finite Z-Transform Pair

A finite z-transform pair has been developed. This pair may be thought of as the discrete analog of the finite Fourier transform (Fourier series). Consider a periodic sequency of period N, i.e., $f(n) = f(n+N)$. Then the transform pair is given by

$$f(n) = \sum_{k=-\infty}^{\infty} E_k \left[\exp(jn \frac{2\pi}{N})\right]^k$$

$$E_k = \frac{1}{N} \sum_{n=0}^{N-1} f(n)\exp(-jnk \frac{2\pi}{N}).$$

Applications of this transform to the parameter variation problem in discrete systems and to the steady-state analysis of sampled data systems with periodic inputs have been made.

J. B. Cruz
W. Perkins

4.19 Optimal Rendezvous Strategies

A study of optimal rendezvous strategies for cooperative controlled systems was completed. The term "rendezvous" is used to mean that the systems approach each other so that the velocities and

accelerations are the same when the positions become the same. A solution to the single-input problem, using the calculus of variations, is given when the performance index is the integrated-square-error plus weighted control. By rewriting the problem in terms of the error coordinates, the rendezvous conditions are replaced by the stability conditions on the Euler-Poisson equations. The stable trajectories are found by factoring the coefficient matrix of the transformed Euler-Poisson equations. By using the stable trajectories, it is possible to express the optimal control laws in terms of the states of the systems. The factorization required to obtain the stable trajectories is, in general, much easier than trying to satisfy the transversality conditions and then deriving the control law.

A solution to the multi-input problem using Pontryagin's Maximum Principle is given for the same performance index. The performance index is rewritten in terms of the stacked state vectors. The rendezvous conditions are adjoined as constraints to the performance index using Lagrange multipliers. Details of this work are found in Report R-218.

D. Gieseking

4.20 Graph Theory

The work on unistor graphs started in the last quarter has been completed.

A unistor is an oriented edge connecting two vertices in a graph. A flow exists in the oriented edge with a value equal to the product of the edge weight and the weight of the initial vertex. The

unistor is characterized by flow, potential, admittance, and directedness--four properties also found in linear equations and electrical networks.

It was shown that a graph of unistors can represent a matrix and the determinant and cofactors can be evaluated by using directed trees and directed 2-trees. The signs of the determinant and cofactors are calculated during the expansion--a separate sign calculation routine is not necessary as it is in some other methods. An extension of the directed tree evaluation method gave a technique for obtaining solutions to a set of simultaneous linear equations.

A technique was established for representing in a node-admittance form an active network by a unistor graph. This graph was then used to determine the values of the unknown voltages of the original circuit.

A vertex potential for a communication net was defined and used to obtain upper and lower bounds on the maximum flow between two vertices of the net. A special class of nets was found for which the terminal capacity can be calculated using unistor graphs.

A complete description of this work is found in Report R-217.

G. Dodd

5. PLATO

D. Bitzer
A. Alpert**
R. A. Avner*
R. Blomme
P. Braunfeld*
E. DeWan
J. Easley*
G. Frampton**
H. Gelder*
W. Golden*
A. Hanson**
B. Hicks
E. R. Lyman
L. Morgan
M. Secrest
S. Singer
R. Suchman*
B. Voth
M. Walker**
R. Whitney**
R. Willson
B. Wilson*

5.1 Introduction

The purpose of the PLATO project has been to develop an automatic computer-controlled teaching system of sufficient flexibility to permit experimental evaluation of a large variety of ideas in automatic instruction including simultaneous tutoring of a large number of students in a variety of subjects. The PLATO system differs from most teaching systems in that the power of a large digital computer is available to teach each student since one such computer controls all student stations. The project work has fallen into three categories, no two of which are wholly separate from each other: (1) development of the tools for research; (2) learning and teaching research; (3) provision of a prototype for multi-student teaching machines.

5.2 PLATO III System Equipment (PLATO Hardware)

During this quarter work continued in the development and construction of circuitry required for the realization of a 20 student station teaching system.

Student station circuitry constructed to date includes all circuitry required for the operation of two student stations. A continuing exemplary effort by various technical sections of the laboratory

*CSL Consultant
**Summer Assistant

dealing with circuit packaging and fabrication suggests that at least a total of 10 student stations will be operable some time in November.

Present interface circuitry has been expanded to include the CSL CSX-1 computer as an alternative computer facility to the CDC 1604. Checkout of the interface was facilitated by a compact general engineering routine written during this quarter by Mr. G. Frampton.

Development continues on special circuitry which will update present circuitry or provide special system facilities. Included in this circuitry is transistor deflection, power control, master keyset, and master video switch circuitry.

B. Voth

5.3 PLATO III Computer Programming (PLATO Software)

5.3.1 The Resident Program for CATO (CATORES).

CATORES has been functional for some time as an input-output monitor for machine language teaching programs communicating with the PLATO III equipment. During this quarter, a careful examination and re-evaluation of the program has taken place with respect to efficient use of the PLATO III equipment, with respect to features suggested by the users as desirable, and with respect to ultimate compatibility with CATO-compiled programs. As a result, the program was almost completely rewritten, with many additions and extensions.

Three different methods of recording student data on magnetic tape are now available. For code-checking, one can now output student data to the printer or to the typewriter as each key is pushed. Elaborate checks have been established to avoid time-consuming storage

tube operations for a student if they are unnecessary. The plot and selective erase routines have been expanded and generalized for easy use with CATO-compiled programs, and several subroutines have been added expressly for use by CATO programs. In addition, the addresses of the subroutine entries and the structures of several internal lists have been modified to meet restrictions imposed by CATO.

Finally, three manually-entered routines have been added. PROGSAVE allows an entire teaching program to be written on an auto-loadable magnetic tape. SPECTRE allows a student's actions to be played back in real time, half time, or double time by executing data read from the student data tape. RESTART allows a program to be continued from the same point at which it was stopped (in case a lesson runs more than one day, or in case of equipment failure). The program uses the data on the data tape to reproduce the exact situation present in memory and on all student screens at the time stoppage occurred.

A comprehensive machine language engineering program was also written in conjunction with the revision of CATORES. This program was used extensively to check and to evaluate the changes to CATORES as they were made and is now used to facilitate the maintenance of the PLATO III equipment.

A. Hanson
M. Walker

5.3.2 DOPEREA. PLATO "dope" is defined as the record of a student's operation of a PLATO keyset. The number of each key pushed is stored on magnetic tape along with its associated time, mode, and

student number. The stored records may be analyzed at a later date in any appropriate fashion. A machine language FORTRAN subroutine, DOPEREA, was written which reads and translates the PLATO "dope" tapes to binary numbers fast enough to allow smooth reading.

M. W. Walker

5.3.3 The CATO (Compiler for Automatic Operations) System.

CATO (Compiler for Automatic Teaching Operations) was completed during the quarter. The system contains three major portions:

FORTBIN - An expanded and modified version of the FORTRAN-60 algebraic compiler for the 1604.

LOGICOMP - A logical compiler which constructs a teaching logic interpretable by CATORES from a vocabulary of 10 directives.

SYSTEMS TAPE - a set of modified subroutines and programs to allow easy use and modification of the system and all programs compiled with it.

S. Singer
A. Hanson

5.4 Plasma Discharge Display Tube Research

The purpose of the research on the plasma discharge display tube is to develop a less expensive replacement for the present PLATO storage tube system. The feasibility of initiating the discharges from outside the tube was tried with excellent success. Controlling the discharge from outside the gas environment not only simplifies construction by allowing the electrodes to be in the external environment, but also effectively adds series impedance to each bulb which helps isolate

each cell from its neighbors. The freedom from adjacency initiated firing will be investigated next quarter, since the firing of adjacent cells should no longer be a problem.

The cell which was used to demonstrate the feasibility of externally controlled discharges was constructed in the following manner. Three glass cover plates 25 mm square by 0.15 mm thick were prepared for use in a vacuum system. On two of these a gold strip 25 mm by 0.127 mm by 100 Å was deposited on the side that was to be on the outside of the cell. The third slide had a 0.127 mm hole drilled in its center. A 0.05 mm thick mylar spacer to channel gas into the cell was placed on either side of the plate with the hole (cell) and the other plates on either side with the gold contacts outwards. The whole assembly was connected to glass tubing with epoxy and filled with neon.

R. Willson

5.5 PLATO Learning and Teaching Research

5.5.1 Inquiry Training (REPLAB). A four week workshop was conducted in June in the College of Education of the University of Illinois to instruct 28 elementary teachers in the use of scientific inquiry classroom techniques. A demonstration class of 22 pupils drawn from the local community was held in conjunction with the workshops. The pupils used the PLATO program, REPLAB (described in an earlier progress report), as one of the lessons in inquiry. The lesson is based on a bimetal strip experiment. No statistical analysis was made of the work of the summer students. For comparison with classroom

behavior many of the workshop teachers monitored the students while they were using PLATO, watched reruns of student performance, or received copies of the "dope" sheets (student records). Interested teachers were also permitted to try the lesson themselves. The rerun of student performance was made possible by a computer program, SPECTRE, which simulates students using PLATO by reconstruction of the operation from the "dope" record stored on magnetic tape during a PLATO lesson.

R. Suchman
E. R. Lyman

5.5.2 Teaching A B C's. Four three-year-old children spent two short sessions on PLATO using ALPHABAT, a program designed to teach the letters of the alphabet. The PLATO equipment was modified to include a semi-automatic audio system. The students were first shown a letter on the screen, told its name, and asked to match it. Later on, they were not shown the letter, but were simply asked to press the key named. The children's reactions and progress gave insight into methods of effective programming for, possible simplifications of, and additions to the PLATO system for use in primary and pre-primary education.

A. Alpert

5.5.3 TEXT TESTER. During the past three months, a new program called TEXT TESTER has been developed. This program is designed to be used in testing new textbooks. The program provides for reproduction of text materials on slides with the insertion of student

answers from the keyboard as in PLATO tutorial logics. The student is permitted wide freedom in the use of the text; therefore, he is allowed to turn pages and to answer questions at random. He is permitted but not required to check answers using a judger which compares students' answers to lists of stored correct answers. Provision is made for the insertion by students of paragraph-form comments about the text materials. Provisions for testing the student at various points throughout the text are also included.

A major feature of this program is the inclusion of "author modes" by which the author may insert or modify correct answers, and insert comments which are intended to help students at specific points in the program, or which are intended to elicit comments from the students.

TEXT TESTER is the first program ready for use with the PLATO Compiler. Code-checking of the TEXT TESTER program will be carried on in September followed by trials of the program with students later in the fall.

J. Easley, Jr.
H. Gelder
W. Golden
B. Wilson

5.5.4 PROOF. During this quarter, work has continued on the preliminary programming and advanced planning of the program for the study of mathematical problem solving (first described in CSL Report R-185).

J. Easley, Jr.
H. Gelder
W. Golden
B. Wilson

6. VACUUM INSTRUMENTATION

D. Alpert
W. Schuemann
L. Simonelli
F. Steinrisser

6.1 Mass Spectrometer Studies

As mentioned in the last progress report, we have obtained a working Davis and Vanderslice mass spectrometer. Its only problem was that the gain of the photomultiplier was about 100 times smaller than expected from factory specifications. The reason was probably an accident during an earlier bakeout, when a glass tube broke, and the system was exposed to air at 250°C. We tried to increase the gain of the photomultiplier by introducing a few grains of $CsNO_3$ into the system and baking it up to 420°C, as many people had done with success. All we observed was a reduced sensitivity of the instrument which can only be explained by distortion of the glass envelope causing a misalignment of the mass spectrometer.

We replaced this mass spectrometer tube by a new one, and baked the zeolite trap and the rest of the system separately. A valve between the system and trap was closed when baking the trap, and the latter was immersed in liquid nitrogen when baking the rest of the system with the valve open. This time, the instrument met the factory specifications.

A Bayard-Alpert gauge with one carbon-free filament and a molybdenum grid purer than usual was added to the system. With the valve to the diffusion pump closed, and the Bayard-Alpert gauge running

at 10 mA, we observed an equilibrium pressure of 4×10^{-10} Torr, the residual gas being mainly He which diffuses through the glass walls, expecially the hot wall of the Bayard-Alpert gauge. Cooling this wall with an air blower reduces the equilibrium pressure to about half the value given above.

We observed a reduced CO partial pressure in our system compared to the one with a Bayard-Alpert gauge with regular electrode material. More experiments are necessary before we can definitely say that this is caused by the absence of carbon in the filament and/or grid.

The softness of this purer electrode material gives mechanical troubles: the filament is bent towards the grid and, without special precautions, touches it easily, and the molybdenum grid is strongly deformed during outgassing.

When the Bayard-Alpert gauge was outgassed with the valve to the pump closed, we do not find the cracking pattern of the pump oil in our mass spectrum. This can be explained by a complete trapping of the backstreaming oil by the zeolite trap. We also find an unexplained dependence of total and partial pressures on the outgassing current. Further experiments are necessary before any conclusions can be drawn.

6.2 Photocurrent Suppressor Gauge

Three modifications of the photocurrent suppressor gauge were tested this quarter. These three plus the previous model are shown for comparison. P_{38} is identical to the original suppressor gauge except that the size of the suppressor had been increased somewhat to give improved suppression characteristics. See Figure 6.1.

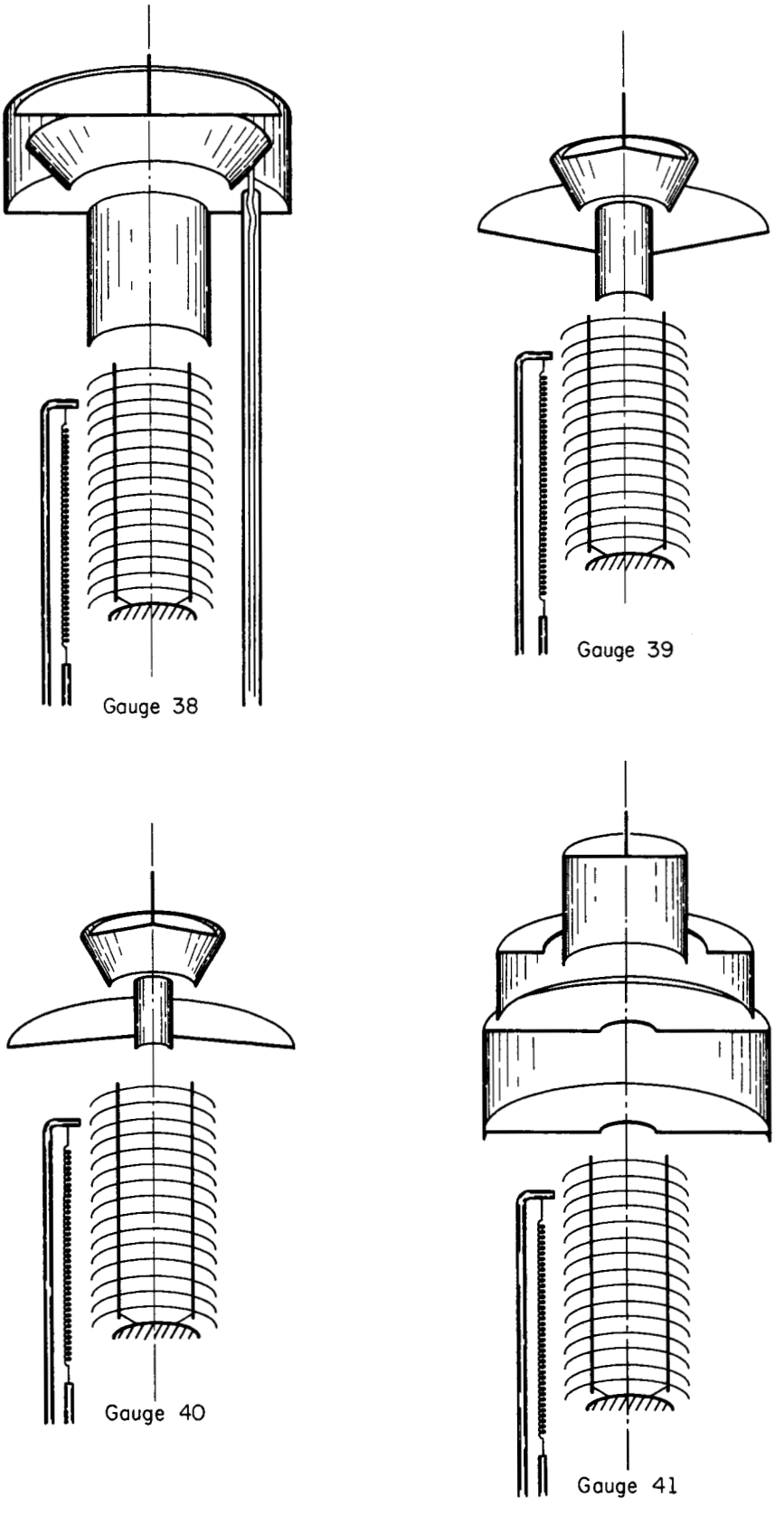

Figure 6.1. Modifications of Photocurrent Suppressor Gauges.

The general purpose of P_{39} and P_{40} was to continue to improve the suppression characteristics and simultaneously to decrease the size of the aperture through which the x-rays pass, before striking the collector, in order to reduce the unsuppressed x-ray limit. A number of interesting conclusions were reached as the result of the tests of these two tubes:

1. The suppressor voltage which is necessary to suppress the x-ray photocurrent can be reduced from 300 volts for the original gauges at 1×10^{-11} Torr to 20 volts by the improved geometry of P_{39} and P_{40}.

2. The x-ray effect due to photoelectrons leaving the suppressor and going to the collector, as the result of x-rays which are reflected from the collector and then strike the suppressor, was increased significantly for tubes P_{39} and P_{40}. In the original suppressor gauges this x-ray limit is in the low 10^{-13} Torr region while in P_{39} and P_{40} it is in the low 10^{-12} Torr region. This increase is undesirable.

3. The sensitivity of the original suppressor gauge was 20 Torr^{-1} with a 3/4" aperture in the shield. P_{39} had a 3/8" aperture and a sensitivity of 15 Torr^{-1}. P_{40} had a 1/4" aperture and a sensitivity of 12 Torr^{-1}. This indeed was surprising and indicates that the focusing in this gauge is extremely good.

With these results, P_{41} was designed. The following advantages of this tube were hoped for:

1. A significant reduction in the unsuppressed x-ray limit due to the geometry changes. Two 3/8" apertures 1-1/8 inches apart are to be used for a shield rather than a short tube. This gives a reduction in the x-ray flux coming through the shield by about a factor of 10 to 100. The two apertures for the shield rather than a tube eliminates any x-rays which would be reflected into the collector region due to reflection from the tube, thereby reducing the unsuppressed x-ray limit.

2. A new suppressor geometry (along with the changes in the shield) makes it impossible for any x-rays to hit the suppressor after one bounce in any place where the resulting photoelectron would go to the collector. This should place the x-ray limit, due to photoelectrons going from the suppressor to the collector, at least a factor of at 10^4 to 10^6 below the unsuppressed x-ray limit, depending on the geometry.

3. The new geometry is much easier to fabricate and align than the previous suppressor gauges.

4. The envelope of P_{41} is fabricated of aluminosilicate glass to make possible lower pressures.

Preliminary data on this tube indicate that the unsuppressed x-ray limit is in the low 10^{-12} Torr region, an improvement by a factor of 100. The sensitivity, however, is down by a factor of 5.

The preliminary data indicate that a study of the focusing properties of these tubes is desirable for two reasons.

1. To make the design of the suppressor gauge more efficient.

2. To examine the possibility of building an unsuppressed gauge with an x-ray limit in the low 10^{-12} Torr region.

This study is now in progress.

6.3 Repairing of Damaged or Unusable Storage Tubes

The PLATO group at C.S.L. uses an expensive Raytheon storage tube in their equipment. For two reasons, these tubes have given the group considerable trouble:

1. The total gas pressure in the tubes is too high, causing the formation of an "ion spot" on the screen, sometimes in as short a time as 10 seconds. This spot both removes the information on the screen in that area and creates a broad white area in the center of the student's monitor.

2. Due to accidents the screen suffers a "burn" which has the characteristic of either not storing or not retaining the information which is written on it. These "burns" were optically visible on the storage screen.

By using several of the tube elements, and with the help of a magnet, it was possible to start a Penning discharge in the tube, which pumped the tubes rather well. With this pump operating, a number of defective tubes were baked at temperatures ranging from $100^{o}C$ to $200^{o}C$, sometimes with the filament on, and sometimes off. All tests

successfully lowered the equilibrium pressure during normal operation to a sufficiently low pressure that the ion-spot formation time is of the order of 3-5 minutes. This processing successfully eliminates the problem of ion spot formation.

In addition, it was noticed that baking the defective tubes seemed to diminish the seriousness of the "burns." Subsequent processing, where the screen was heated to 350°C and the gun to 150°C for an extended time with the Penning discharge on, has resulted in the complete repair of one tube, and it has been returned to service. An interesting fact is that the optically visible "burn" disappears during processing. Further experiments are proceding on the "burn" repair problem.

6.4 Impact Ionization Studies

During this quarter, work has continued on the impact ionization of adsorbed gases on surfaces due to electron bombardment.

CO has been put on a moly sample, and its maximum cross section for impact ionization determined to be about 6×10^{-6} ions/electron. The temperature of desorption for the adsorbed CO is about 800°C.

When oxygen was placed on a platinum sample, the yield of ions/electron was less than 10^{-8}. If the filament of the Bayard-Alpert was left on (giving a conversion of O_2 to CO), the yield increased to 6×10^{-7}. The gas layer was desorbed at about 200°C. The values for CO were 6×10^{-7} and 200°C also, indicating that the CO is adsorbed on the surface in both cases.

The amount of CO on the surface seems to be a small fraction of a monolayer because (1) flashing the sample gives a very small increase in the pressure, and (2) the time required to saturate the effect when gas is being introduced is much less than that required by a monolayer. Further studies using an all-metal system are in progress.

7. PLASMA PHYSICS

M. Raether
J. K. Aggarwal
A. Barger
H. Bohmer
W. Carr
J. Crowder
B. Hicks
T. Lie
C. Mendel
H. G. Slottow
M. A. Smith
R. Hosken

7.1 The Boltzmann Equation for a Shock Wave

We developed an algebraic theory of shock wave structure in the previous quarter. A draft of a report on the algebraic theory was finished and sent to Professor Yen at AVCO, who will be one co-author, for his comments. The theory, within the limitations imposed by the nature of the basic assumptions, covers all Mach numbers and any monatomic gas.

There have been two applications. The first application was to the calculation of shock structures for the full range of Mach numbers, from one to infinity, for a gas of elastic spheres. Direct comparisons between the results of the algebraic theory, the Mott-Smith theory, and Navier-Stokes theory are possible. A second application of the algebraic theory was in the analysis of production runs with the Monte Carlo program. This use of the theory indicates that the Monte Carlo calculations are converging too slowly, and that one high-order boundary condition is not being satisfied with adequate accuracy.

In an attempt to study convergence of the Monte Carlo program, without interference from the statistical fluctuations, we ran fifty iterations with a fixed collision sample at each station. These runs

were made with 10^4 collisions/sample, five stations, and a Mach number of 2.5. No clear convergence was indicated, possibly because there is an interaction between the rate of convergence and the large statistical fluctuations corresponding to these small samples. A similar but less extensive run for a larger sample also did not clearly show adequate convergence properties. In this more accurate calculation, however, the period of the long-term fluctuations during the iterations was decreased by a factor of two or more.

In view of these several indications of convergence troubles, and the recommendations of Dr. Mott-Smith regarding methods of integration, it seemed appropriate to redesign the integration method. A new method has therefore been derived which imposes a least-square fit of the derivative of a polynomial, for each station, to the Monte Carlo derivatives df/dn at each interior point of the shock, and requires exact matching of the polynomial to the boundary values of f. Proper choice of the degree of the polynomials will force a certain smoothing of the "noisy" values of the derivatives calculated by Monte Carlo. Fitting in the manner described to the interior values of the derivative and to the end values of the function makes step-wise integration, with its danger of instability, unnecessary. We believe that a second step toward improving the integration method will make fitting of a polynomial for each velocity bin subject to auxiliary conditions expressing the fact that three moments of the derivatives vanish at each station in the shock wave.

While these revisions of the program are being made, we shall undertake a very simple calculation for a "pseudo-shock" that was suggested by Arnold Nordsieck as a test of his Monte Carlo method.

B. Hicks

7.2 Oscillations in Non-Uniform Plasmas

In the previous quarter we reported observations of incoherent scattering of microwaves by a high frequency mode of a finite non-uniform plasma. Although a number of papers have appeared during the last two years that discuss certain features of these modes, the whole subject is still in its infancy.[1-6]

In the following, we outline a method that permits us to treat one special case of a non-uniform plasma in considerable detail, and that provides a suitable basis for the investigation of more general cases.

We consider a one-dimensional plasma enclosed between two infinite, specularly reflecting walls at $x = 0$ and $x = L$. The behavior of the plasma is described by the linearized Vlassov and Poisson equations

$$\frac{\partial f_1}{\partial t} + v \frac{\partial f_1}{\partial x} - \frac{e}{m} E_1 \, n(x) \frac{\partial f_o}{\partial v} = 0, \tag{1}$$

$$\frac{\partial E_1}{\partial x} = -4\pi e \int f_1 dv \, . \tag{2}$$

The term $E_o \partial f_1 / \partial v$ can be shown to be small, and it will be neglected henceforth. As boundary conditions, we require

[1] The papers cited here are listed in the Bibliography (§7.3).

$$f(0,v) = f(0,-v),$$
$$f(L,v) = f(L,-v), \tag{3}$$

$$E(0) = E(L) = 0. \tag{4}$$

Following Weissglas we introduce the functions $F^+ = f(v) + f(-v)$ and $F^- = f(v) - f(-v)$. The boundary condition for the distribution function now simply requires $F^- = 0$ at the boundaries. The functions f and E are assumed to have a time dependence of $e^{i\omega t}$. Equations (1) and (2) then become

$$F^- + \frac{v^2}{\omega^2}\frac{\partial^2 F^-}{\partial x^2} + 2i\,\frac{e}{m\omega}\,n(x)\,E_1\,\frac{\partial f_o}{\partial v} = 0, \tag{5}$$

$$\frac{\partial}{\partial x}\left\{E_1 + \frac{4\pi e i}{\omega}\int_o^\infty F^-\,v\,dv\right\} = 0. \tag{6}$$

If no external driving field is present, equation (6) implies

$$E_1 = -\frac{4\pi e i}{\omega}\int_o^\infty F^-\,v\,dv\,. \tag{7}$$

For F^- and E_1, we now choose the following expansions which satisfy the boundary conditions:

$$F^- = \Sigma\, F_k \sin(\pi kx/L); \quad E_1 = \Sigma\, E_k \sin(\pi kx/L). \tag{8}$$

For n(x) we choose the special profile

$$n(x) = n_o(1 + \nu\cos 2\pi x/L). \tag{9}$$

It will be shown later that this choice is less restrictive than it might appear. Inserting (8) and (9) into (5) and (7) results in the following recurrence relation for E_k:

$$\epsilon_k E_k + \frac{\nu}{2}(\epsilon_k - 1)E_{k-2} + \frac{\nu}{2}(\epsilon_k - 1)E_{k+2} = 0 \qquad (10)$$

with

$$\epsilon_k = 1 + \frac{\omega_p^2 L}{\pi k} \int_{-\infty}^{+\infty} \frac{(\partial f_o/\partial v)dv}{\omega - \pi k v/L} .$$

For k = 1 we have to observe that $E_{-1} = -E_1$. These are two infinite sets of homogeneous equations, for odd and even indices.

For a solution to exist, the determinants must vanish. This requires

$$0 = \begin{vmatrix} \epsilon_1 - \frac{\nu}{2}(\epsilon_1 - 1) & \frac{\nu}{2}(\epsilon_1 - 1) & 0 & 0 & \cdots \\ \frac{\nu}{2}(\epsilon_3 - 1) & \epsilon_3 & \frac{\nu}{2}(\epsilon_3 - 1) & 0 & \cdots \\ 0 & \frac{\nu}{2}(\epsilon_5 - 1) & \epsilon_5 & \frac{\nu}{2}(\epsilon_5 - 1) & \cdots \\ 0 & 0 & \cdots & \cdots & \cdots \\ \cdots & \cdots & \cdots & \cdots & \cdots \end{vmatrix} \qquad (11)$$

and

$$0 = \begin{vmatrix} \epsilon_2 & \frac{\nu}{2}(\epsilon_2 - 1) & 0 & 0 & \cdots \\ \frac{\nu}{2}(\epsilon_4 - 1) & \epsilon_4 & \frac{\nu}{2}(\epsilon_4 - 1) & 0 & \cdots \\ 0 & \frac{\nu}{2}(\epsilon_6 - 1) & \epsilon_6 & \frac{\nu}{2}(\epsilon_6 - 1) & \cdots \\ 0 & 0 & \cdots & \cdots & \cdots \\ \cdots & \cdots & \cdots & \cdots & \cdots \end{vmatrix} \qquad (12)$$

In order to evaluate these determinants we divide the k^{th} row by $\frac{\nu}{2}(\epsilon_k - 1)$. The odd determinant then becomes

$$0 = \begin{vmatrix} \frac{2\epsilon_1}{\nu(\epsilon_1-1)} - 1 & 1 & 0 & 0 & \cdots \\ 1 & \frac{2\epsilon_3}{\nu(\epsilon_3-1)} & 1 & 0 & \cdots \\ 0 & 1 & \frac{2\epsilon_5}{\nu(\epsilon_5-1)} & 1 & \cdots \\ \cdots & \cdots & \cdots & \cdots & \cdots \end{vmatrix},$$

and a corresponding expression holds for the even set. The determinant is of the form

$$D = \begin{vmatrix} a_1 & 1 & 0 & 0 & \cdots \\ 1 & a_2 & 1 & 0 & \cdots \\ 0 & 1 & a_3 & 1 & \cdots \\ \cdots & \cdots & \cdots & \cdots & \cdots \end{vmatrix}.$$

We divide the first row by a_1 and subtract it from the second row. This yields

$$D = a_1 \begin{vmatrix} 1 & 1/a_1 & 0 & 0 & \cdots \\ 0 & a_2 - 1/a_1 & 1 & 0 & \cdots \\ 0 & 1 & a_3 & \cdots & \cdots \\ \cdots & \cdots & \cdots & \cdots & \cdots \end{vmatrix}.$$

Proceeding in this fashion we obtain

$$D = a_1(a_2-1/a_1)(a_3 - \frac{1}{a_2-1/a_1})(a_4 - \frac{1}{a_3 - \frac{1}{a_2-1/a_1}})\cdots \quad .$$

By calculating the partial numerators and denominators of these continued fractions it can be shown that all terms cancel except for the numerator of the last continued fraction. Hence

$$D = \lim_{n\to\infty} A_n \, ,$$

where A_n is the numerator of

$$a_n - \frac{1}{a_{n-1} - \frac{1}{a_{n-2} - \cdots}} \, .$$

If this continued fraction vanishes, we may write

$$0 = a_1 - \frac{1}{a_2 - \frac{1}{a_3 - \cdots}} \, . \tag{13}$$

This is the dispersion relation in the non-uniform case.

A particularly simple expression for the continued fraction arises if we replace ϵ_k by its value derived from the moment equations for a warm plasma

$$\epsilon_k = 1 - \frac{\omega_p^2}{\omega^2 - (\pi k v_T/L)^2} \, . \tag{14}$$

Inserting this expression into (10), we notice that the recurrence relation for the E_k is identical with that for the coefficients of the Mathieu functions $se_n(x,q)$, if we put[7]

$$a = \frac{L^2}{\lambda_D^2}\left(\frac{\omega^2}{\omega_p^2} - 1\right); \quad q = \frac{\nu}{2}\frac{L^2}{\lambda_D^2}; \quad \lambda_D = \frac{\pi v_T}{\omega_p} .$$

Hence, we conclude that E obeys a Mathieu equation

$$E'' + (a - 2q\cos 2\pi x/L)E = 0 .$$

The eigenmodes of oscillation are then given by the corresponding values of a and q, belonging to the Mathieu function $se_n(x,q)$. The corresponding eigenfunction E_n is the Mathieu function $se_n(x,q)$.

The qualitative behavior of these eigenvalues is sketched in Figure 7.1. We notice the asymmetry for positive and negative values of q corresponding to the two different density profiles (Figure 7.2).

The eigenvalues can of course be calculated exactly by using the correct expression for the dielectric constant and solving for the roots of (13). Computer calculations in this direction are in progress. Likewise, the eigenfunctions corresponding to the modes can be obtained numerically.

The knowledge of the eigenfunction and eigenvalues provides a starting point for the calculation of more difficult density profiles by perturbation theory, because the near degeneracy of the eigenvalues for $\nu = 0$ has been removed.

E. Jackson
M. Raether

7.3 Bibliography

[1] A. Dattner, Phys. Rev. Letters 10, 205 (1963).

[2] J. C. Nickel, J. V. Parker and R. W. Gould, Phys. Rev. Letters 11, 183 (1963).

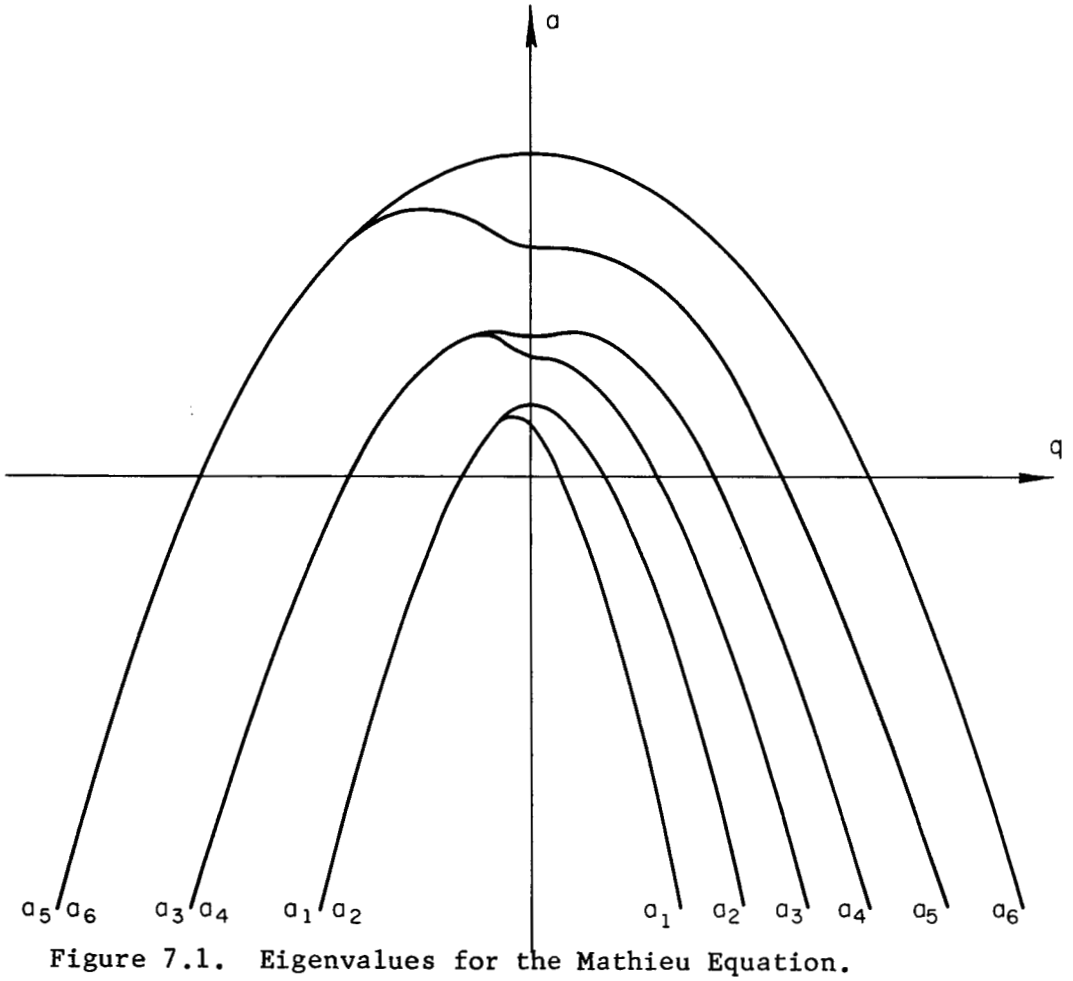

Figure 7.1. Eigenvalues for the Mathieu Equation.

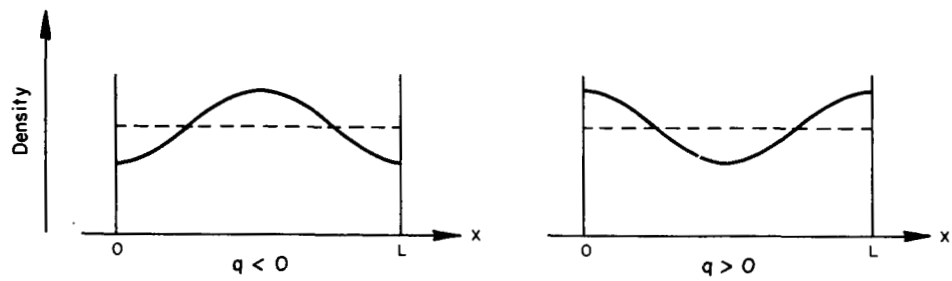

Figure 7.2. Plasma Density Profiles

[3]S. J. Buchsbaum and A. Hasegawa, Phys. Rev. Letters 12 685 (1964).

[4]P. Weissglas, Phys. Rev. Letters 10, 206 (1963). (This paper also contains numerous references to earlier work.)

[5]P. Weissglas, J. Nucl. Energy - Part C, 6, 251 (1964).

[6]F. C. Hoh, Phys. Rev. 133, A1016 (1964).

[7]McLachlan, Theory and Application of Mathieu Functions (Oxford, 1951).

8. HIGH MAGNETIC FIELD SUPERCONDUCTORS

C. B. Satterthwaite
J. O. Kopplin
W. O. Gentry
R. Bernstein
R. Ries
R. Klingbiel
M. G. Craford

8.1 Introduction

This group is primarily interested in studies which contribute to an understanding of the persistence of superconductivity to very high magnetic fields. Studies include materials preparation, investigations of the properties of Type II superconductors, and the properties of superconducting specimens of very small dimensions.

8.2 Superconductivity in Thallium-Antimony Alloys

In an attempt to find a Type II superconductor with a transition temperature near the lambda-transition of liquid He, the superconducting properties of a series of thallium-antimony alloys have been studied. The series contained alloys of composition between 0 and 30 atomic percent of antimony.

The samples were prepared in an inert atmosphere and heat treated for several hours to attain homogeneity. The transition temperatures were obtained from magnetization studies using the vibrating sample magnetometer. From these measurements were also obtained the critical fields Hc, Hc_1, and Hc_2 characterizing the Type II superconductivity in these alloys. Measurements of the residual resistance ratio were also made.

Residual resistivity measurements indicate that in the neighborhood of 13.5 atomic percent Sb an ordered structure must occur. Also in this region of composition there is a distinct rise in the transition temperature, though the maximum occurs between 15 and 18.5 atomic percent.

The alloys were Type II superconductors, but they were far from ideal in that their magnetization was highly irreversible, and there was appreciable trapping of flux.

This program has been terminated for the time being with the completion of a Master's thesis, the termination of Mr. Gentry's tenure as an industrial research fellow, and his return to the Fansteel Metallurgical Corporation. A report will be forthcoming.

W. Gentry

8.3 Superconducting Tunneling

The anomalous current peaks in tunneling characteristics of Nb-Nb oxide-In junctions, reported in the previous QPR, have been studied in some detail. This structure has now been observed in a number of junctions composed of a variety of superconductors, and it is now believed to be characteristic of junctions exhibiting a DC supercurrent resulting from either a tunneling supercurrent (the dc Josephson effect) or a low critical current superconducting short.

In situations where two superconductors are separated by a thin insulating barrier, we know from Josephson and others that one can transfer Cooper pairs at zero-voltage from one side to the other

without change of energy. At finite voltages, however, the transfer involves a change of energy $2e\Delta V$ per pair, where ΔV is the voltage difference between the two sides, and the transfer is allowed only if there is an absorption mechanism for photons of this energy.

A current at a finite voltage in excess of the quasi-particle tunneling current is then evidence of such an absorption process and is a manifestation of what has come to be known as the AC Josephson effect.

In Figure 8.1 the peak structure in the current-voltage curves is shown relative to the normal two-superconductor tunneling characteristic.

To resolve the structure, which represents a whole series of negative resistance regions, we resorted to the circuit shown in Figure 8.2. With the parts of the circuit indicated immersed in liquid He, it was possible to provide a very low impedance source for the tunneling current. The load line, which is numerically equal to $R_1 + R_2$, could be made as low as a few milliohms, thus allowing us to resolve very sharp current peaks.

Tunneling current peaks at finite voltages have been observed under a number of circumstances, and it is possible to make some generalizations about them.

1. The current peaks at finite voltages always accompanied a super-current peak at zero voltage and were of comparable magnitude. Similar structure was observed whether the zero-voltage current was a

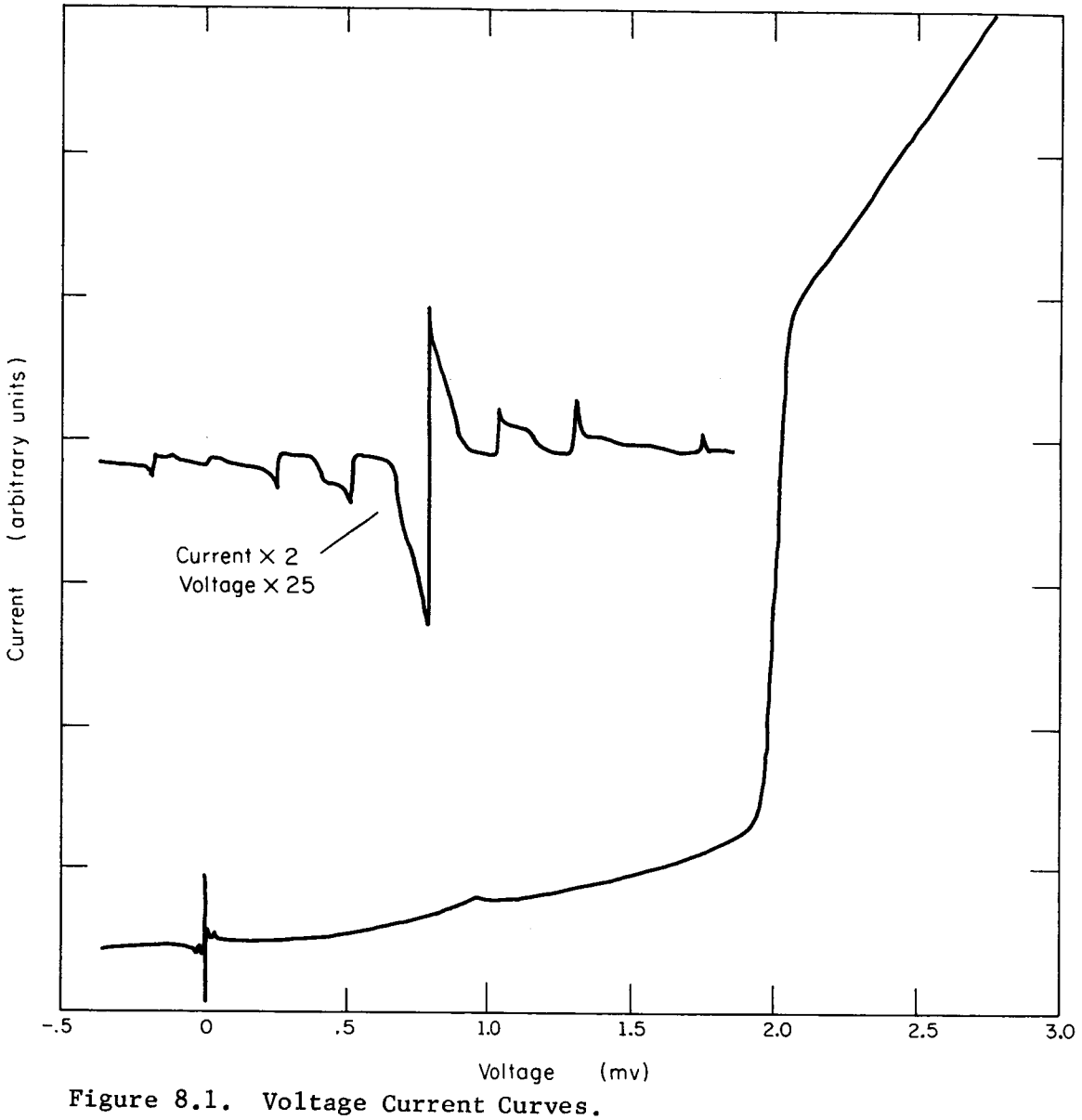

Figure 8.1. Voltage Current Curves.

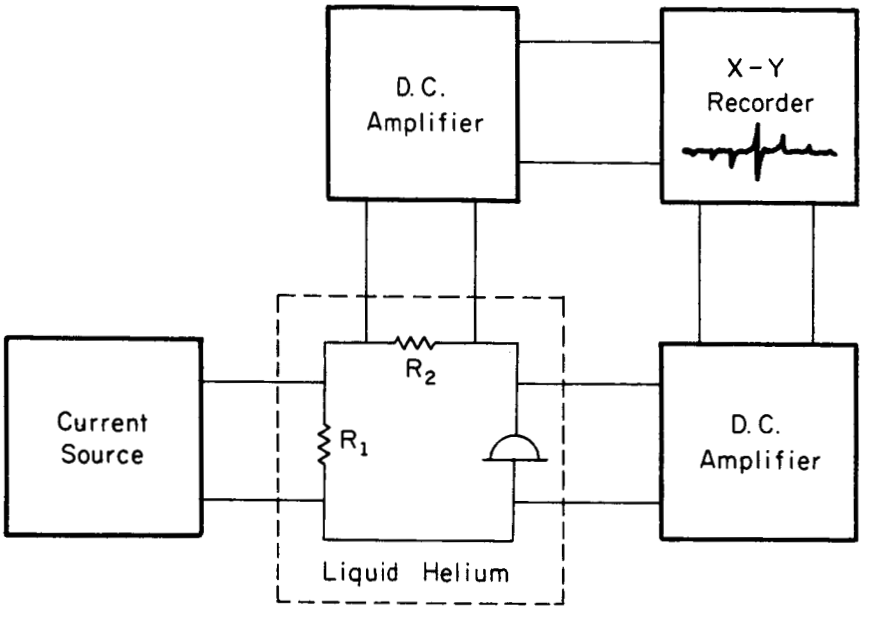

Figure 8.2. Circuit for Measuring Tunneling Current.

Josephson tunneling current or a low critical-current superconducting short. This is not unreasonable, since the two are, in many ways, the same. It is clear that if a voltage can be sustained across either, the transport of pairs must be accompanied by an absorption process. The shorts could be easily distinguished: (a) they had no magnetic field dependence, (b) the currents at zero-voltage were greater than the theoretical maximum for the DC Josephson effect, and (c) there appeared to be an appreciable normal conductance parallel to the tunneling current.

2. Variation of temperature affected the structure in two ways. First, the number and amplitude of the peaks increased with decreasing temperature. This corresponds to the enhancement of the Josephson effect or the increase in the critical current of a short with decreasing temperature. The second effect is that the voltages at which the peaks occur are shifted uniformly with variation of temperature. The shifts in voltage with temperature variation for both Nb-NbO_x-In and Nb-NbO_x-Sn junctions, relative to the transition temperatures of In and Sn, are shown in Figure 8.3.

3. In cases where the current peaks accompanied superconducting shorts, the structure was independent of magnetic field, but when they accompanied Josephson tunneling the amplitude of all peaks were periodic in magnetic field and with approximately the period of the zero-voltage peak. They were, however, not necessarily in phase with it or with each other. This is evident from Figure 8.4, which shows curves for the same junction at a series of magnetic fields.

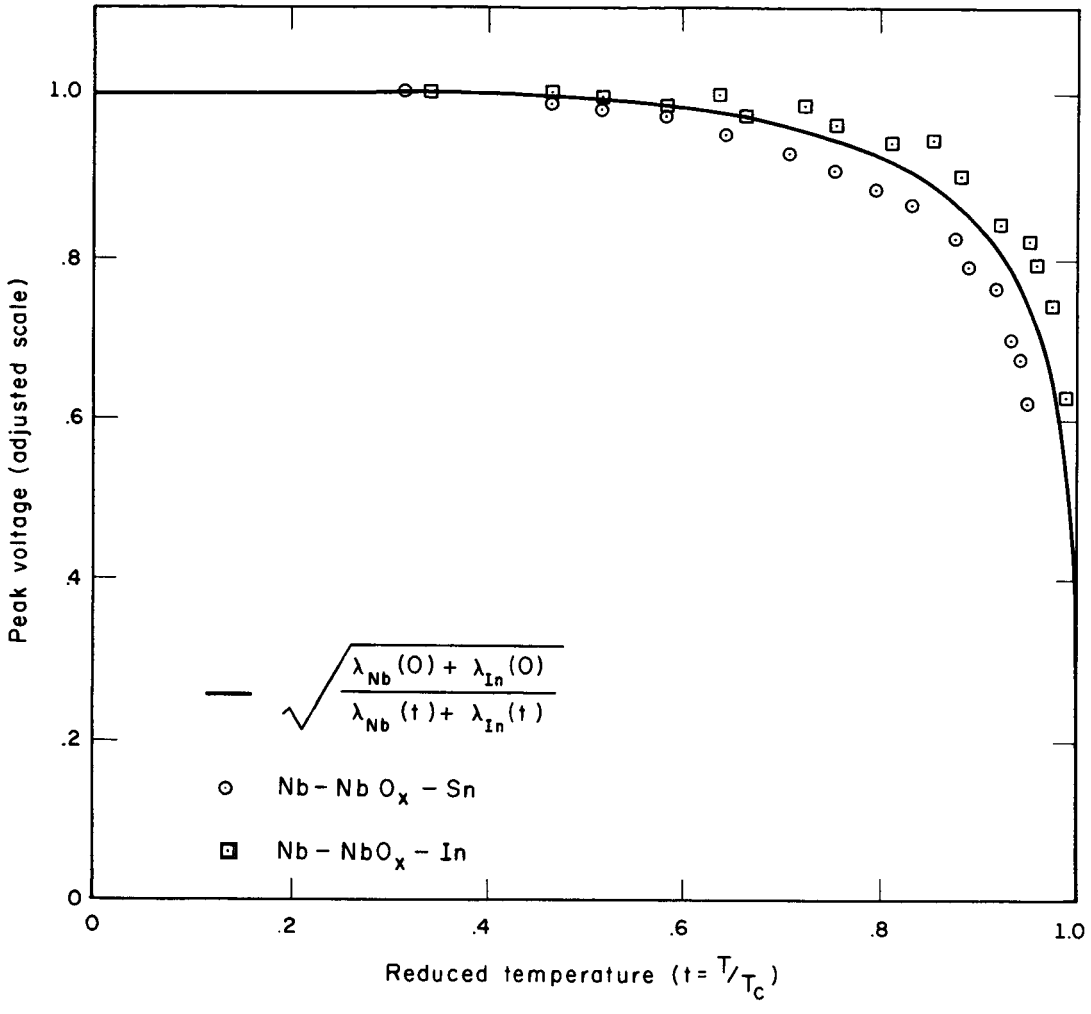

Figure 8.3. Temperature Dependence for Voltages for the Peaks in the Josephson Current.

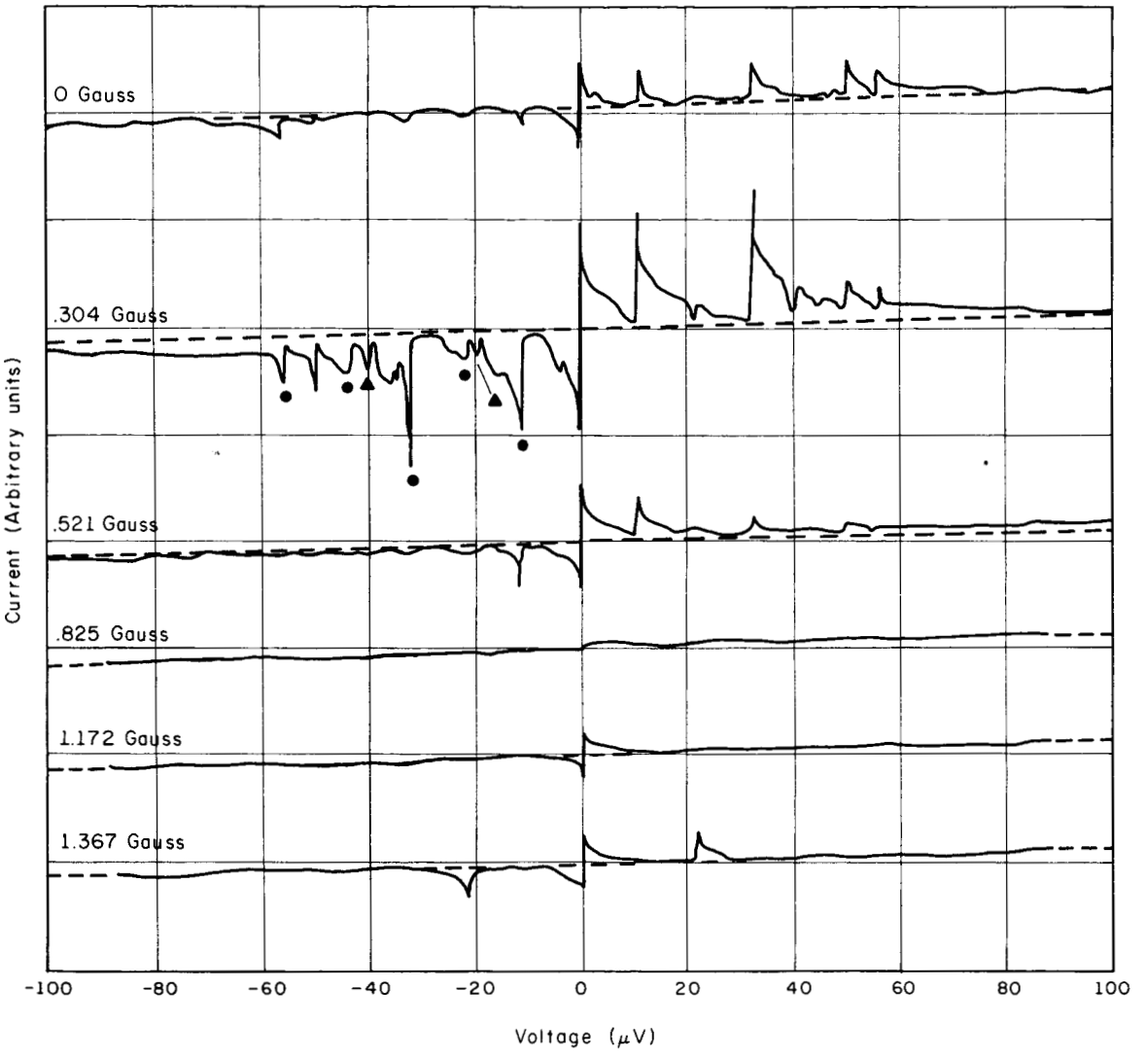

Figure 8.4. Magnetic Field Dependence for the Structure of the Peaks in the Josephson Current.

In most of the junctions there appeared to be series of peaks at multiples of a fundamental frequency. For example, the series of peaks indicated with circles in Figure 8.4 is spaced at multiples of approximately 10.7 microvolts; the first three peaks occur quite accurately at this spacing. Those peaks marked with triangles form another series at 20 and 40 microvolts.

It appears that the structure we observed is very similar to the steps in the tunneling curves observed by Fiske. These have been analyzed by Fiske and his co-workers as standing wave modes in the junction itself. Treating the junction as a transmission line which has a capacitance per unit length, determined by the thickness and dielectric constant of the insulating barrier, and an inductance per unit length, determined by the penetration depths, they have been able to calculate standing wave frequencies of the magnitude observed. One gets from a treatment of this kind a temperature dependence of the voltage at which the peaks should occur, resulting from the temperature dependence of the penetration depth.

The voltage at which the peaks should occur is inversely proportional to $\sqrt{(\lambda_{Nb} + \lambda_X)}$ where λ_{Nb} is the penetration depth of Nb and λ_X is the penetration depth of the other superconductor, In or Sn in the present case. Therefore, the ratio of the voltage at any temperature t to the limiting value V_o, as the reduced temperature t approaches zero, is $V/V_o = \sqrt{[(\lambda_{Nb}(0) + \lambda_X(0))/(\lambda_{Nb}(t) + \lambda_X(t))]}$. Inserting values for the penetration depths of Nb and In and their

temperature dependences one obtains the theoretical curve shown in Figure 8.3. The theoretical curve for Nb-Sn is not appreciably different from the one shown.

M. Craford
R. Peacock
R. Ries
C. Satterthwaite

8.4 Micro-micro Voltmeter

A trial version of a cryogenic, low level DC voltmeter has been constructed and is being tested. Sensitivity and other operating characteristics are being studied.

The voltage sensitivity of this instrument is primarily due to its unique input circuitry. The input of the voltmeter consists of a small solenoid which is vibrated inside of a set of pickup coils. A sensitive AC amplifier and lock-in detection system, connected to the pickup coils, detect the presence of any DC current in the solenoid. The entire input circuit is operated in a liquid helium bath, allowing the use of superconducting wire in the solenoid and pickup coil.

The input impedance is therefore purely inductive, so that extremely small DC voltages can be detected. The voltage must be large enough compared to the input inductance so that the measurement can be made in a reasonable length of time, and the source impedance must be below some minimum level, however.

Preliminary measurements indicate the sensitivity to be quite high, although considerable difficulty is encountered from spurious signals. The main spurious signals are apparently caused by

poor shielding of both the earth's field and the AC fields at the instrument's carrier frequency. One microampere in an inductance of 200 μH is presently detectable, although superimposed upon spurious signals equivalent to a 100 μA input. With this sensitivity, and source resistances of 10^{-7} ohm or less, one picovolt (10^{-12} volt) would be detectable in about three minutes, and would be well above the noise in twenty minutes.

R. Ries

8.5 Crystallization of Nb_3Sn

Considerable progress has been made toward growing Nb_3Sn single crystals of sufficient size for the study of their properties. Crystals with flat faces up to 2 mm on an edge have been obtained.

A total of ten runs has been completed using the Nb_3Sn crystal-growing furnace. The duration of these runs varied from 19 hours to 160 hours. In all cases a niobium-tipped rod was inserted into the Nb-Sn solution to provide the site for nucleation of the crystals. This produced polycrystalline starts as numerous crystals were obtained from each run. Figure 8.5 shows the niobium tip and Nb_3Sn crystals as taken from the furnace following run number 5. The solution temperature, in this case, was held at 1286°C and the initial tip temperature was 1220°C. The solution was stirred magnetically and the tip was in contact with the solution for a total of 43 hours. Figure 8.6 shows a single crystal after being isolated and removed from the tip.

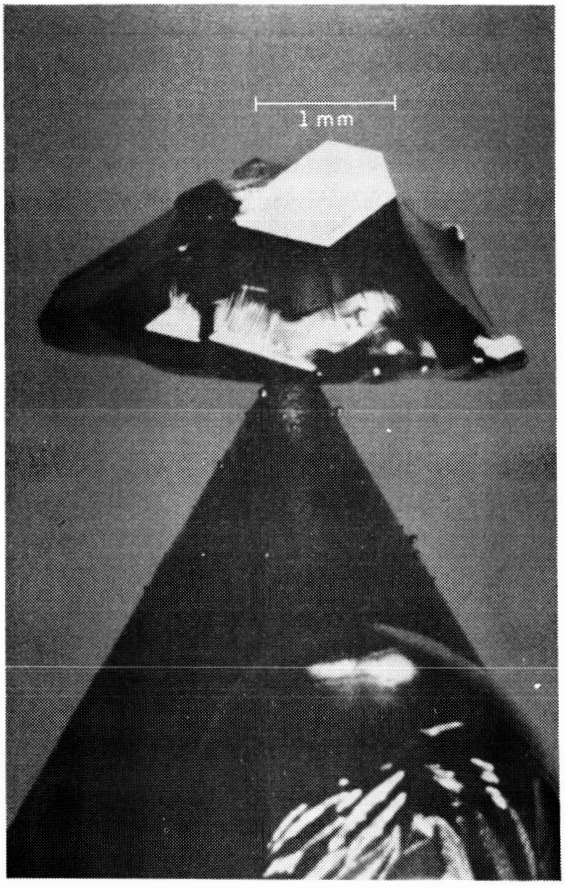

Figure 8.5. Nb_3Sn Crystals as Withdrawn from Furnace.

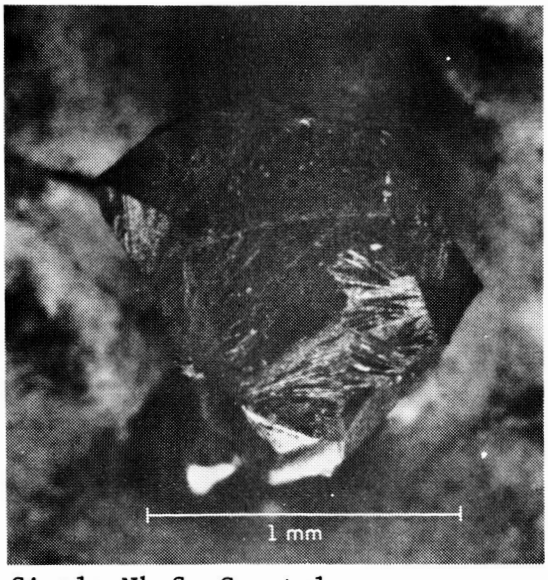

Figure 8.6. Single Nb_3Sn Crystal.

Correlation between crystal structure and size with the various furnace parameters has been limited because of failure and/or necessary modification of certain furnace parts. All crystals have been grown from a molten Nb-Sn solution held at a temperature of approximately 1290°C with a maximum temperature variation of 2°C during the crystal growing period. Withdrawal or raising of the niobium tip during the crystal growing period at any rate approaching .0075 inches per hour was detrimental in that only a high number of very imperfectly structured crystals were obtained. Rotation of the tip at 12 rpm resulted in the growth of larger crystals with fewer structural imperfections.

A schematic diagram of the furnace is shown in Figure 8.7. The Nb-Sn solution is contained in a high purity alumina crucible supported in the hot zone of the furnace by a lava pedestal. A pt/pt 13% Rh thermocouple adjacent to the silicon-carbide heating element was used to control the furnace temperature, and thermocouples inside the niobium tip and in a ceramic tube inserted into the solution were used to measure the tip and solution temperatures, respectively. A slight flow of argon was established and maintained through the furnace during the crystal growing period after the furnace chamber had been evacuated using a standard vacuum pump.

The next phase of the investigation will use small Nb_3Sn crystals for top-seeding the Nb-Sn solution. The problem here is securing the rather small crystals in a manner which will withstand the

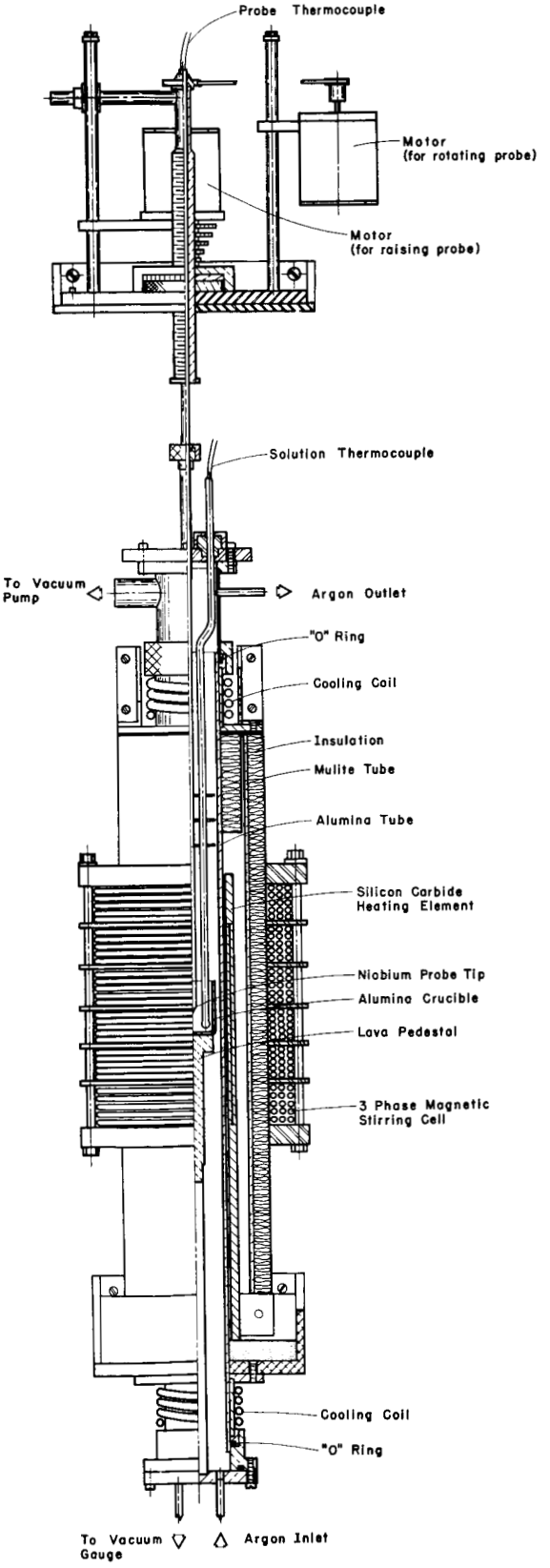

Figure 8.7. Furnace for Growing Nb_3Sn Crystals.

high furnace temperature. Attention will be given to determining if there is a preferred crystallographic orientation for growth of the crystals. Also, studies of the purity, structure, electrical and magnetic properties of the crystals are planned.

Work on the chemical analysis of solution samples taken from the furnace, for the purpose of determining the solubility of niobium in tin in the 1100-1300°C temperature range, has continued, but final results have not been obtained. Considerable time was spent developing a cerate titration technique using nickel as a reductor for the stannic tin solution, only to cast doubt on the suitability of the nickel reductor for the quantitative determination of tin in this system.

J. Kopplin
R. Klingbiel

9. HIGH VOLTAGE BREAKDOWN

D. Alpert, T. Casale, D. Lee
E. M. Lyman, H. Tomaschke, W. Edelstein

9.1 Critical Field for Tungsten Electrodes

The data for broad-area parallel-tungsten electrodes in ultrahigh vacuum have been presented in the form of Fowler-Nordheim plots. The slope of these plots yields the enhancement factor β by which the average or gross electric field V/d at the cathode must be multiplied in order to obtain the local field present at the tips of the whiskers responsible for the field emission current. The final result for the average value of the critical field E_b at breakdown is $6.5 \pm 1 \times 10^7$ V/cm, which agrees very well with the results of Dyke et al.,[1] Boyle, Kisliuk, and Germer,[2] Gofman et al.,[3] and Tomaschke.[4] Preliminary results were reported in the CSL Progress Report for June, July, and August, 1962, where it was shown that the critical field thus obtained is constant within the experimental error for over five orders of magnitude of gap spacing. The value of E_b may thus be

[1] Dyke, Trolan, Marten, and Barbour, Phys. Rev. 91, 1043 (1953).

[2] Boyle, Kisliuk, and Germer, Journ. Appl. Phys. 26, 720 (1955).

[3] Gofman, Protopopov, and Shuppe, Soviet Phys. Solid State Physics 2, 1203 (1960).

[4] H. Tomaschke. PhD. Thesis, University of Illinois, Urbana. (1964).

regarded as a characteristic property of the electrode material. A very important consequence of this result is that the value of breakdown voltage is thus related to, and directly predictable from, the observed volt-ampere characteristic of the predischarge field emission current when the work function φ is known. Knowing the critical electric field at which breakdown will occur, one can arrive in a non-destructive way at the value of voltage at which breakdown will occur. Another important result is that under clean conditions, the breakdown characteristics for electrodes of a given material are apparently independent of the geometry, and of whether the electrodes are single crystal or polycrystalline in structure.

9.2 Multiple Points on Broad Electrodes

In our broad area electrode experiments, the predischarge current was found to arise from a number of point emitters on the cathode. As the voltage between the electrodes is slowly raised, at a current of about one microampere, the electron beams impinging on the anode produce sharply defined blue-green pin points of light on the anode. The light is very faint and requires dark adaptation to be observed. The brightness of the spots increases with increasing current, and they number from 1 to 10 per cm^2. For an electrode spacing of about 0.4 cm (V = 160 kV, I = 150 μA), their diameter is approximately 0.01 cm. Although the spot pattern is relatively unvarying over a period of hours, certain spots may disappear or flicker and new spots appear elsewhere from time to time, either with or without visible breakdown, the total number remaining roughly constant, at a given gap

spacing. It was observed that a lateral movement of the cathode with respect to the anode (maintaining constant gap spacing) caused the entire pattern of spots to move across the anode in conjunction with the cathode motion. Thus it seems plausible to attribute each individual spot to the beam from an individual whisker or protrusion on the cathode. The size of the anode spots agrees with that calculated by the method of Vibrans[5] for the beam spreading from a whisker of the dimensions observed by Tomaschke and others.[6] The light intensity from the spots is roughly that to be expected from the visible tail of the bremsstrahlung spectrum of the impinging electrons, as suggested by Silverman and Vibrans,[7] or from "Lilienfeld" radiation.[8]

When the high voltage was initially applied to electrodes which had not been exposed to high voltage for a period of a day or so, fluorescent spots which did not move laterally in conjunction with the cathode motion were seen at the anode. Spots were also seen on the cathode. These fluorescent spots were of somewhat different color than the spots produced by the impinging electron beams. They completely disappeared in a minute or so, and are presumably due to specks

---

[5] G. E. Vibrans, Lincoln Laboratories Technical Report 308 (18 April 1963).

[6] Little and Whitney, NRL Report No. 5944 (May 20, 1963) and Journ. Appl. Phys. 34, 2430 (1963).

[7] E. Silverman, Lincoln Laboratory (MIT). High Power Tube Program Semiannual Report (December, 1962).

[8] See, for example: H. Boersch, C. Radeloff, and G. Sauerbrey, Phys. Rev. Letters 7, 52 (1961).

of fluorescent material adhering to the anode and cathode; their disappearance is associated with gas bursts and sharp initial current pulses, which also disappear in a short time after applying the high voltage.

9.3 Effect of Gas on the Predischarge Current

Previous experiments were repeated in an attempt to obtain a reproducible measurement on the effect of gas in reducing the predischarge current between tungsten electrodes. Although a reduction of two orders of magnitude in the current was observed, presumably due to the blunting by ion bombardment of the emitter tips, the experiments were regarded as unsuccessful, because the results were not reproducible. The trouble seemed to be due to a masking of the gap emission current by an ion current which takes the longest discharge path (from flange to flange) in the electrode chamber, and builds up by the Townsend mechanism. The apparatus is being modified with guard rings to isolate the ion current from the gap current.

9.4 Predischarge Current and Voltage Breakdown between Gold Electrodes

Gold electrodes of purity 99.95 have not given the degree of reproducibility in predischarge current and voltage breakdown that were obtained with the single crystal tungsten electrodes. Nevertheless, straight Fowler-Nordheim plots are obtained, and the enhancement factors derived from the plots in conjunction with the observed breakdown voltages indicate a preliminary characteristic electric field intensity

at breakdown, E_b, of $6.4 \pm 1 \times 10^7$ V/cm, which is nearly the same as that obtained for tungsten. (ϕ = 4.8 eV was assumed for gold.)

9.5 Flicker and Rectangular Pulses

It was previously reported[9] that the field emission current from both small and broad area electrodes exhibits "rectangular" fluctuations as if some of the emission sites were bistable in their emission properties. The duration of the pulses ranges from microseconds to seconds, or even longer. Then, it was observed that in both types of electrodes the light spots on the anode due to impinging electron beams fluctuate in intensity, or flicker. When observed on a modified field emission microscope, the flicker was found to consist of the appearance and disappearance of small bright spots within the pattern of a single emitter point.

By focusing the light from a flicker spot onto a photocell, it was found that the emission current fluctuates in exact correspondence with the light.

Several attempts were made to eliminate the flicker. Cooling the cathode support wires with a liquid helium bath produced no observable change in the flicker, nor did cleaning the cathode by heating it to temperatures as high as 2400°C.

In order to obtain a purer material, a tungsten cathode was heated in the presence of tungsten carbonyl vapor, causing the tungsten carbonyl to decompose and deposit a layer of pure tungsten on the cathode. This reduced but did not eliminate the flicker.

---

[9] CSL Progress Report for Dec., 1963, Jan. and Feb., 1964, p.74. Also Progress Report for March, April, May, 1964, p.89.

However, with a cathode made of ultrahigh purity tungsten (obtained from the Westinghouse Electric Corporation) no flicker whatever was observed, even when the voltage was increased to the point of breakdown.

On the basis of this single preliminary observation, one may postulate that the flicker is due to the diffusion out of the bulk and migration across the surface of the tungsten on the part of impurity atoms. As these atoms hop onto and off of an emission site they alter the work function and hence the emission current, thereby creating the flicker effect. Further work with ultrahigh purity tungsten is in progress to check this tentative hypothesis.

10. THIN FILMS

R. N. Peacock
M. G. Craford
J. T. Jacobs
R. E. Zelac
W. P. Bleha
A. Jones

10.1 Tin Oxide Films

The report for the previous quarter discussed transparent conducting tin oxide films and gave results of various measurements which were made to learn something of the electronic structure of this material. Measurements were reported on the temperature coefficient of resistance, stability, and the effects of gaseous and vacuum ambients on conductivity. To learn more about the structure, the transient photoconductivity has been measured with visible and with ultraviolet light. Analysis of this data is under way at present. Preliminary results show that the band gap in this material may be larger than the energy corresponding to the shortest ultraviolet light used.

J. Jacobs

10.2 Hard Superconducting Films

Attempts made earlier this year to deposit films of vanadium and niobium on substrates at room temperature, even under good vacuum conditions, did not produce films having normal superconducting properties. Transition temperatures, when they were found, were far below the bulk values. Using heated substrates, films of V and Nb have been made recently which have superconducting transition temperatures similar to bulk material.

The method used for heating the substrates, although unusual, has given good results. Substrates are customarily heated by placing them in contact with a heated metal or graphite block, or by using infrared heaters. When these heaters consume large amounts of power, they outgas themselves and adjacent portions of the evaporation system, and at best do not insure that the substrate has the required constant, uniform temperature. The substrates used in making the superconducting films were of quartz 1/16" X 3/8" X 1-1/2" with about 2000 Å of titanium on the back side. This titanium film served as an ohmic heating element in perfect thermal contact with the substrate. Outgassing was negligible, and, since the power consumption was small, there was no heating of the remainder of the system. A temperature of 600°C was obtained, using about 40 V at 0.5 A, or only 20 watts. In testing, temperatures as high as 1000°C were possible without destruction of the Ti film.

The phenomenon of superconductivity has served in this case to show the large difference in the structure of films deposited at different substrate temperatures. The ability to make good films of superconductors will be useful in future experiments.

W. Bleha

10.3 Epitaxial Films

The vacuum system to be used for these studies was completed at the start of this quarter, and pressures as low as 1×10^{-10} Torr were obtained. Titanium sublimation pumping, when properly used, was quite successful in maintaining a low total pressure in the system.

In the operation of this system an unusual amount of trouble was encountered with copper-gasketed seals leaking after bakeout, and considerable time has been lost for this reason. Other baked systems in the laboratory, using the same flanges, have not had this problem.

Only tin films have been studied so far, and these were deposited on cleaved NaCl substrates which had been baked in vacuum before cleavage. The aim of these experiments is to produce highly oriented single-crystal films. Electron-diffraction and electron-microscope examination of some tin films has shown that they consist of oriented polycrystalline films at best, and do not have the desired uniform structure. It is possible that the use of thicker films, higher or lower pressures during deposition, or better outgassing of the tin charge could lead to better results. Substrate temperature is an important parameter, of course.

R. Zelac

10.4 Luminescent Films

The usual luminescent screens in cathode-ray tubes are made by a settling process which can be performed only by a specially skilled technician, if uniform screens are to be made. At best, they have irregularities which limit resolution. Such screens also evolve, into the vacuum, various active gases harmful to surface experiments. Evaporated luminescent screens, which have been made by a number of workers, do not suffer from these difficulties, and would be useful to a number of projects in this laboratory.

Suitable screens usually cannot be made simply by vapor-depositing a normal phosphor. Evaporation may destroy the activator, or stoichometry, or both. Heat treatment after deposition can restore luminescence. Selection of phosphor materials is important for this method.

Films of $CaWO_4$ were recently deposited and successfully activated by heating in air, although the process was not completely reproducible. Experiments with this, and with other phosphors, will continue. Rare earth oxides, which can have luminescent properties, may be promising according to some reports.

W. Bleha

11. COMPUTER OPERATIONS

H. G. Slottow
C. Arnold
S. Chilton
G. Crawford
L. Hedges
J. Knoke
V. Metze
R. Nash
E. Neff
J. Stifle

11.1 Introduction

This group is responsible for the development and operation of the CSL computing facility.

11.2 CSX-1 Computer

11.2.1 Operations

Period: June 3, 1964, to September 3, 1964

Total running time:	859.3 hrs.
Ave. per day (7 day week):	9.44 hrs.
Operational Time: 99%	850.8 hrs.
Scheduled Maintenance Time:	0.0 hrs.
Emergency Maintenance Time:	8.5 hrs.

Breakdown of emergency maintenance time:

8.0 hrs: replace 25 volt power supply

0.33 hrs: replace shorted transistor (2N2270)

0.17 hrs: replace diode that was installed backwards

J. Stifle

11.2.2 Modifications

Eight additional interrupt channels have been added to the computer.

Additional equipment has been added to facilitate communication between the CSX-1 and the 7094.

Additional input-output circuitry has been added to allow the PLATO experiment access to the CSX-1.

J. Stifle
R. Trogdon

11.3 CDC 1604 Computer

11.3.1 Operations

Period: June 1, 1964, to August 31, 1964

Total running time:		1049.9 hrs.
Ave. per day (7 day week)		11.41 hrs.
Operational Time:	95.25%	1000.00 hrs.
Preventive Maintenance Time:	4.56%	47.9 hrs.
Emergency Maintenance Time:	0.19%	2.00 hrs.

Breakdown of emergency maintenance time:

2.00 hrs: Intermittent memory failure.

E. Neff

11.3.2 Systems Programming

A new resident system is being prepared for the CDC 1604 computer. The assembler for the system, now almost complete, contains most of the features of FAP. In addition, it contains a more flexible expression evaluator, allowing the use of parenthesis, and a compile pseudo operation. Descriptions of this and other programs in the system will be published as they are completed.

R. Nash
S. Seshu

Distribution list as of September 1, 1964

1 Director
Air University Library
Maxwell Air Force Base, Alabama
Attn: CR-4803a

1 Redstone Scientific Information Center
U.S. Army Missile Command
Redstone Arsenal, Alabama

1 Electronics Research Laboratory
University of California
Berkeley 4, California

2 Hughes Aircraft Company
Florence and Teale
Culver City, California
Attn: N.E. Devereux
Technical Document Center

3 Autonetics
9150 East Imperial Highway
Downey, California
Attn: Tech. Library, 3041-11

1 Dr. Arnold T. Nordsieck
General Motors Corporation
Defense Research Laboratories
6767 Hollister Avenue
Goleta, California

1 University of California
Lawrence Radiation Laboratory
P.O. Box 808
Livermore, California

1 Mr. Thomas L. Hartwick
Aerospace Corporation
P.O. Box 95085
Los Angeles 45, California

1 Professor Zorab Kaprelian
University of Southern California
University Park
Los Angeles 7, California

1 Sylvania Electronic Systems-West
Electronic Defense Laboratories
P.O. Box 205
Mountain View, California
Attn: Documents Center

1 Varian Associates
611 Hansen Way
Palo Alto, California 94303
Attn: Technical Library

1 Huston Denslow
Library Supervisor
Jet Propulsion Laboratory
California Institute of Technology
Pasadena, California

1 Professor Nicholas George
California Institute of Technology
Electrical Engineering Department
Pasadena, California

1 Space Technology Labs., Inc.
One Space Park
Redondo Beach, California
Attn: Acquisitions Group
STL Technical Library

2 Commanding Officer and Director
U.S. Navy Electronics Laboratory
San Diego, California 92052
Attn: Code 2800, C.S. Manning

1 Commanding Officer and Director
U.S. Navy Electronics Laboratory
San Diego, California 92052

1 Commanding Officer
Office of Naval Research Branch Office
1000 Geary Street
San Francisco, California 94109

1 The RAND Corporation
1700 Main Street
Santa Monica, California
Attn: Library

1 Stanford Electronics Laboratories
Stanford University
Stanford, California
Attn: SEL Documents Librarian

1 Dr. L.F. Carter
Chief Scientist Air Force
Room 4E-324, Pentagon
Washington 25, D.C.

1 Mr. Robert L. Feik
Associate Director for Research
Research and Technology Division
AFSC
Bolling Air Force Base 25, D.C.

1 Captain Paul Johnson (USN-Ret)
National Aeronautics and Space
Administration
1520 H. Street, N.W.
Washington 25, D.C.

1 Major Edwin M. Myers
Headquarters USAF (AFRDR)
Washington 25, D.C.

1 Dr. James Ward
Office of Deputy Director
(Research and Info)
Department of Defense
Washington 25, D.C.

1 Dr. Alan T. Waterman
Director, National Science Foundation
Washington 25, D.C.

1 Mr. G.D. Watson
Defense Research Member
Canadian Joint Staff
2450 Massachusetts Ave., N.W.
Washington 8, D.C.

1 Mr. Arthur G. Wimer
Chief Scientist
Air Force Systems Command
Andrews Air Force Base
Washington 25, D.C.

1 Director Advanced Research
Projects Agency
Washington 25, D.C.

1 Air Force Office of Scientific Research
Directorate of Engineering Sciences
Washington 25, D.C.
Attn: Electronics Division

1 Director of Science and Technology
Headquarters, USAF
Washington 25, D.C.
Attn: AFRST-EL/GU

1 AFRST - SC
Headquarters, USAF
Washington 25, D.C.

1 Headquarters, R & T Division
Bolling Air Force Base
Washington 25, D.C.
Attn: RTHR

1 Headquarters, U.S. Army Materiel Command
Research Division, R & D Directorate
Washington 24, D.C.
Attn: Physics and Electronics Branch
Electronics Section

1 Commanding General
U.S. Army Materiel Command
Washington 25, D.C.
Attn: R & D Directorate

1 Commanding Officer
Diamond Ordnance Fuze Laboratories
Washington 25, D.C.
Attn: Librarian, Room 211, Bldg. 92

1 Operations Evaluation Group
Chief of Naval Operations (OP-13EG)
Department of Navy
Washington, D.C. 20350

1 Chief of Naval Operations (Code OP-07T)
Department of the Navy
Washington , D.C. 20350

1 Commanding Officer
U.S. Army Personnel Research Office
Washington 25, D.C.

1 Commanding Officer & Director
Code 142 Library
David W. Taylor Model Basin
Washington, D.C. 20360

1 Chief, Bureau of Ships (Code 686)
Department of the Navy
Washington, D.C. 20360

1 Chief, Bureau of Ships (Code 732)
Department of the Navy
Washington, D.C. 20360

1 Chief, Bureau of Naval Weapons
Technical Library, DLI-3
Department of the Navy
Washington, D.C. 20360

1 Director, (Code 5140)
U.S. Naval Research Laboratory
Washington, D.C. 20390

1 Chief of Naval Research (Code 437)
Department of the Navy
Washington, D.C. 20360

1 Dr. N. Wallace Sinaiko
Institute for Defense Analyses
Research & Engineering Support Division
1666 Connecticut Ave., N.W.
Washington 9, D.C.

1 Data Processing Systems Division
National Bureau of Standards
Conn. at Van Ness
Room 239, Bldg. 10
Washington 25, D.C.
Attn: A.E. Sellow

1 National Bureau of Standards
Research Information Center &
Advisory Service on Information
Processing
Data Processing Systems Division
Washington 25, D.C.

1 Exchange and Gift Division
The Library of Congress
Washington 25, D.C.

1 NASA Headquarters
Office of Applications
400 Maryland Avenue, s.w.
Washington 25, D.C.
Attn: Mr. A.M. Greg Andrus
Code FC

1 APGC (PGAPI)
Eglin Air Force Base
Florida

1 Martin Company
P.O. Box 5837
Orlando, Florida
Attn: Engineering Library
MP-30

1 Commanding Officer
Office of Naval Research, Branch Office
230 North Michigan
Chicago , Illinois 60601

1 Laboratories for Applied Sciences
University of Chicago
6220 South Drexel
Chicago, Illinois 60637

1 Librarian
School of Electrical Engineering
Purdue University
Lafayette, Indiana

1 Donald L. Epley
Department of Electrical Engineering
State University of Iowa
Iowa City, Iowa

1 Commanding Officer
U.S. Army Medical Research Laboratory
Fort Knox, Kentucky

2 Keats A. Pullen, JR.
Ballistic Research Laboratories
Aberdeen Proving Ground, Maryland

1 Director
U.S. Army Human Engineering Laboratories
Aberdeen Proving Ground, Maryland

1 Mr. James Tippett
National Security Agency
Fort Meade, Maryland

1 Commander
Air Force Cambridge Research Laboratories
Laurence G. Hanscom Field
Bedford, Massachusetts

1 Dr. Lloyd Hollingsworth
Director, ERD AFCRL
L.G. Hanscom Field
Bedford, Massachusetts

1 Data Sciences Laboratory
Air Force Cambridge Research Lab.
Office of Aerospace Research, USAF
L.G. Hanscom Field
Bedford, Massachusetts
Attn: Lt. Stephen J. Kahne - CRB

1 Instrumentation Laboratory
Massachusetts Institute of Technology
68 Albany Street
Cambridge 39, Massachusetts
Attn: Library M1-109

1 Research Laboratory of Electronics
Massachusetts Institute of Technology
Cambridge 39, Massachusetts
Attn: Document Room 26-327

1 Dr. Robert Kingston
Lincoln Laboratories
Lexington, Massachusetts

1 Lincoln Laboratory
Massachusetts Institute of Technology
P.O. Box 73
Lexington 73, Massachusetts
Attn: Library, A-082

1 Sylvania Electric Products, Inc.
Electronic Systems
Waltham Labs. Library
100 First Avenue
Waltham 54, Massachusetts

1 Minneapolis-Honeywell Regulator Co.
Aeronautical Division
2600 Ridgeway Road
Minneapolis 13, Minnesota
Attn: Dr. D.F. Elwell
Main Station : 605

1 Inspector of Naval Material
Bureau of Ships Technical Representative
1902 West Minnehaha Avenue
St. Paul 4, Minnesota

20 Activity Supply Officer, USAELRDL
Building 2504, Charles Wood Area
Fort Monmouth, New Jersey
For: Accountable Property Officer
Marked: For Inst. for Exploratory Research
Inspect at Destination
Order No. 576-PM-62-91

1 Commanding General
U.S. Army Electronic Command
Fort Monmouth, New Jersey
Attn: AMSEL-RE

1 Miss F. Cloak
Radio Corporation of America
RCA Laboratories
David Sarnoff Research Center
Princeton, New Jersey

1 Mr. A.A. Lundstrom
Bell Telephone Laboratories
Room 2E-127
Whippany Road
Whippany, New Jersey

1 AFMDC (MDSGO Maj. F. Wheeler, Jr.)
Holloman Air Force Base
New Mexico 88330

1 Commanding General
White Sands Missile Range
New Mexico

1 Microwave Research Institute
Polytechnic Institute of Brooklyn
55 John Street
Brooklyn 1, New York

1 Cornell Aeronautical Laboratory, Inc.
4455 Genesee Street
Buffalo 21, New York
Attn: J.P. Desmond, Librarian

1 Sperry Gyroscope Company
Marine Division Library
155 Glen Cove Road
Carle Place, L.I., New York
Attn: Mrs. Barbara Judd

1 Major William Harris
RADC (RAWI)
Griffiss Air Force Base
New York

1 Rome Air Development Center
Griffiss Air Force Base
New York
Attn: Documents Library
RAALD

1 Library
Light Military Electronics Department
General Electric Company
Armament & Control Products Section
Johnson City, New York

1 Columbia Radiation Laboratory
Columbia University
538 West 120th Street
New York 57, New York

1 Mr. Alan Barnum
Rome Air Development Center
Griffiss Air Force Base
Rome, New York

1 Dr. E. Howard Holt
Director
Plasma Research Laboratory
Rensselaer Polytechnic Institute
Troy, New York

3 Commanding Officer
U.S. Army Research Office (Durham)
Box CM, Duke Station
Durham, North Carolina
Attn: CRD-AA-IP, Mr. Ulsh

1 Battelle-DEFENDER
Battelle Memorial Institute
505 King Avenue
Columbus 1, Ohio

1 Aeronautical Systems Division
Navigation and Guidance Laboratory
Wright-Patterson Air Force Base
Ohio

1 Aeronautical Systems Division
Directorate of Systems Dynamic Analysis
Wright-Patterson Air Force Base
Ohio

1 Commander
Research & Technology Div.
Wright-Patterson Air Force Base
Ohio 45433
Attn: MAYT (Mr. Evans)

1 Commanding Officer (AD-5)
U.S. Naval Air Development Center
Johnsville, Pennsylvania
Attn: NADC Library

2 Commanding Officer
Frankford Arsenal
Philadelphia 37, Pennsylvania
Attn: SMUFA-1300

1 H.E. Cochran
Oak Ridge National Laboratory
P.O. Box X
Oak Ridge, Tennessee

1 U.S. Atomic Energy Commission
Office of Technical Information Extension
P.O. Box 62
Oak Ridge, Tennessee

1 President
U.S. Army Air Defense Board
Fort Bliss, Texas

1 Director
Human Resources Research Office
The George Washington University
300 North Washington Street
Alexandria, Virginia

20 Defense Documentation Center
for Scientific & Technical Information
Cameron Station
Alexandria, Virginia 22314

1 Commander
U.S. Army Research Office
Highland Building
3045 Columbia Pike
Arlington 4, Virginia

1 U.S. Naval Weapons Laboratory
Computation and Analysis Laboratory
Dahlgren, Virginia
Attn: Mr. Ralph A. Niemann